

A real-time, event-triggered storm surge forecasting system for the state of North Carolina

Craig Mattocks ^{*,1}, Cristina Forbes ¹

University of North Carolina at Chapel Hill, Institute for the Environment, CB# 1105, 100 Miller Hall, Chapel Hill, NC 27599-1105, USA

ARTICLE INFO

Article history:

Received 23 November 2007

Received in revised form 24 June 2008

Accepted 27 June 2008

Available online 23 July 2008

Keywords:

Storm surge

Hurricane

Event-triggered

Forecasting system

ADCIRC

Coastal ocean model

Gradient wind vortex

Tidal forcing

Surface roughness length

North Carolina

ABSTRACT

A new real-time, event-triggered storm surge prediction system has been developed for the State of North Carolina to assist emergency managers, policy-makers and other government officials with evacuation planning, decision-making and resource deployment during tropical storm landfall and flood inundation events. The North Carolina Forecast System (NCFS) was designed and built to provide a rapid response assessment of hurricane threat, accomplished by driving a high-resolution, two-dimensional, depth-integrated version of the ADCIRC (Advanced Circulation) coastal ocean model with winds from a synthetic asymmetric gradient wind vortex. These parametric winds, calculated at exact finite-element mesh node locations and directly coupled to the ocean model at every time step, are generated from National Hurricane Center (NHC) forecast advisories the moment they are inserted into the real-time weather data stream, maximizing the number of hours of forecast utility. Tidal harmonic constituents are prescribed at the open water boundaries and applied as tidal potentials in the interior of the ocean model domain. A directional surface roughness parameterization that modulates the wind speed at a given location based on the types of land cover encountered upwind, a forest canopy sheltering effect, and a spatially varying distribution of Manning's-n friction coefficient used for computing the bottom/channel bed friction are also included in the storm surge model. Comparisons of the simulated wind speeds and phases against their real meteorological counterparts, of model elevations against actual sea surface elevations measured by NOAA tide gauges along the NC coast, and of simulated depth-averaged current velocities against Acoustic Doppler Current Profiler (ADCP) data, indicate that this new system produces remarkably realistic predictions of winds and storm surge.

© 2008 Elsevier Ltd. All rights reserved.

1. Introduction

North Carolina, with 20 counties bordering the ocean, is particularly prone to hurricanes because the eastern end of the state juts out into the Atlantic Ocean and the Gulf Stream. There were 50 direct hits on North Carolina from 1851 to 2006 (Table 10, [Blake et al., 2007](#)), of which 13 were major hurricanes (intensity breakdown: 24 of Category 1 strength, 14 Category 2, 11 Category 3, 1 Category 4, no Category 5 storms). The highest death totals were primarily a result of a rise in the ocean surface elevation (storm surge) of 10 ft or greater associated with many of these major hurricanes.

In addition, North Carolina faces a difficult evacuation challenge due to the large numbers of tourists who flock to the Outer Banks during the summer and the narrow, two-lane rural roads that lead

out of these areas. Estimates of the peak tourist population and the time required to evacuate the NC coast ([Capitol Broadcasting Company, 2006](#)) range from 9 h for Pender County (with a peak tourist population of 35,000) to 28 h for Hyde County (with a peak tourist population of 5200). These evacuation clearance times are grossly underestimated because they are based on an extrapolated Year 2000 census. Brunswick County, for example, now boasts a peak tourist population near 350,000 instead of the 190,000 used in computing an evacuation time of 12 h. Evacuation is not a linear process, it slows down dramatically with moderate increases in population. In addition, the number of vehicles fleeing coastal communities jumps by 50% when the intensity of a storm increases from Category 1–2 to 3–5 strength. The original traffic studies crudely assumed that one county would evacuate at a time when, in reality, an exodus from multiple counties at once will jam Interstate 40 and the smaller state highways that feed it ([Williams et al., 2005](#)). Also, no allowance was made for flooding ahead of a storm, which often inundates access roads leading to the main traffic arteries. Some estimates set the required evacuation times for Brunswick and New Hanover counties to well over 30 h. Since

* Corresponding author. Tel.: +1 252 726 6841x154; fax: +1 252 726 2426.

E-mail address: cmattock@email.unc.edu (C. Mattocks).

¹ Present address: University of North Carolina at Chapel Hill, Institute of Marine Sciences, 3431 Arendell St., Morehead City, NC 28557, USA.

emergency managers prefer not to issue evacuation orders at night, a lead time of at least 36 h is desired for evacuating the barrier islands.

Another threat from tropical storms is coastal erosion along North Carolina's fragile barrier islands. Recent storms, such as Hurricane Isabel in 2003 and Hurricane Ophelia in 2005, breached the protective beach dunes and cut new inlets through the islands in a matter of hours, demolishing buildings and severing state highways in the process. The loss of sand alone costs the federal and state governments millions of dollars each year for beach renourishment and for dredging to re-open ship navigation channels. Along Bogue Banks, for example, over 8.5 million cubic yards of sand have been pumped in from offshore in the past 6 years to maintain the beach along the 25-mile island (Carteret County Shore Protection Office, 2007). The NC Coastal Resources Commission uses erosion rates calculated every 5 years from aerial photographs to set strict limits on the setback distance allowed for new construction along the oceanfront. The Coastal Area Management Act (CAMA) prevents rebuilding along sensitive waterways designated as Areas of Environmental Concern (AEC) when the width of an eroded plot of land becomes too narrow. Thus, the loss of even a few feet of shoreline to coastal storms can result in millions of dollars of economic damage to the real estate and construction industries.

To address these challenges, the North Carolina Forecast System (NCFS) was created to assist emergency managers, policy-makers and government officials in evacuation planning, decision-making and resource deployment during tropical storm landfall and flood inundation events. The prediction of storm surge along coastal North Carolina due to hurricane activity is the primary focus of the system. The NCFS utilizes a computationally optimized, parallelized version of the ADCIRC coastal ocean circulation/storm surge prediction model for this purpose, coupled with an analytical asymmetric gradient wind model.

This publication is organized as follows. The ADCIRC storm surge prediction model and the asymmetric vortex wind forcing are described in Section 2. Next, the NCFS operational workflow and its three modes of operation are explained in Section 3. Section 4 presents operational storm surge prediction results for Tropical Storm Ernesto (2006). Incorporation of the directional surface roughness, Manning's-n friction coefficient and forest canopy parameterizations into ADCIRC to increase its accuracy is chronicled in Section 5. Finally, in Section 6, a validation of the winds, predicted sea surface elevations and current velocities for Hurricane Ophelia (2005) is carried out to assess the performance of the model enhancements with hurricane-forced winds.

2. NCFS components

2.1. ADCIRC storm surge prediction model

ADCIRC is an unstructured grid, finite-element hydrodynamic model used to simulate storm surge, tides and riverine flow. The model is well documented, both in the published scientific literature and on the ADCIRC web site (<http://adcirc.org/>). It has been used extensively for tidal prediction (Westerink, 1993; Westerink et al., 1992; Westerink et al., 1993; Blain and Rogers, 1998) and storm surge prediction (Blain et al., 1994; Dietsche et al., 2007; Luettich et al., 1996; Blain and McManus, 1998; Lynch et al., 2004; Gruber et al., 2006). The two-dimensional, depth-integrated version employed in the NCFS, ADCIRC-2DDI, model solves a vertically integrated continuity equation for water surface elevation. Spurious oscillations associated with a primitive Galerkin finite-element formulation of this equation are prevented by utilizing the generalized wave continuity equation (GWCE). The vertically

integrated momentum equations are solved to determine the depth-averaged ocean current velocity.

The NCFS model grid domain (Fig. 1a), which extends from 97.85° to 60.04°W and from 7.90° to 45.83°N, encompasses the Western Atlantic, the Gulf of Mexico and the Caribbean Sea.

The unstructured computational mesh was created at UNC's Institute of Marine Sciences (UNC-IMS) by enhancing and merging several pre-existing grids. It consists of 227,240 nodes and 440,904 elements in the NCFS configuration and allows higher horizontal resolution in areas where it is needed (Fig. 1b), ranging from tens of kilometers offshore to tens of meters through channels and inlets (minimum mesh size is 27 m). The bathymetry (Fig. 1c) was interpolated from the Eastcoast 2001 grid (Mukai et al., 2002) and augmented with data from the National Geophysical Data Center's Coastal Relief Model (CRM), which has a horizontal resolution of 3 arc-seconds (90 m). Higher-resolution representations of several inlets and estuaries, constructed from NOAA National Ocean Service hydrographic soundings, were carved into the larger scale bathymetry (Hench and Luettich, 2003). Topography from the NC Floodplain Mapping Program's 6 m resolution LiDAR digital elevation model (DEM) was used in the northern half of North Carolina. All data were converted to the mean water level (MWL) vertical datum (Feyen et al., 2006).

2.2. Synthetic asymmetric vortex wind forcing

The primary objective of the NCFS is to provide a quick, reasonably accurate assessment of storm threat to the NC coast with the maximum number of hours of forecast utility possible. The choice of wind data for initializing and forcing the ADCIRC storm surge model is critical in determining the system's ability to produce storm surge forecasts in the minimum amount of wall clock time. A detailed investigation of NHC's forecast products, their generation, availability, timing and accuracy and real-time sources of wind data available through the Local Data Management (LDM) server and NHC's anonymous ftp server was conducted. The decision was made to develop an event-triggered system composed of a synthetic asymmetric Holland (1980) gradient wind model that could be used to construct a tropical storm vortex from the NHC forecast advisories that enter the LDM Family of Services (FOS) real-time weather data stream and couple it directly to the ADCIRC storm surge prediction model.

This approach has several important operational advantages. First, it allows a forecast simulation to be launched as soon as a forecast advisory is issued by NHC, sometimes 10–20 min before the official release time, instead of waiting up to several hours for the National Center for Environmental Prediction (NCEP) North American Mesoscale (NAM) model winds to become available, plus an additional 1–2 h required for downloading and pre-processing the surface wind and pressure data. Second, synthetic asymmetric vortex winds can be generated on-the-fly from the gradient wind formula, so they can be directly coupled to the ocean model at every time step while the model is running. In fact, to optimize performance, the parametric wind model has been embedded in ADCIRC. Since these parametric winds are available at perfect analytical resolution and true intensity, they can be calculated at the exact locations of the ADCIRC model's computational nodal points in the finite-element mesh. In contrast, the gridded NCEP NAM winds have a comparatively coarse horizontal resolution of 4–36 km and must be interpolated to model nodes in both space and time. This may introduce error and can cause along-track elliptical distortions in the shape of the isolachs, resulting in an artificially weak representation of the storm and its attendant wind stress, especially for fast-moving tropical cyclones (Westerink et al., 2008).

An ADCIRC simulation initialized with synthetic asymmetric vortex winds provides a quick-look, rapid-response storm surge

forecast that can serve as the first member of an ensemble of sea surface elevation simulations. Other hurricane wind forecasting systems, such as the parametric wind model employed by Xie et al. (2006) and the WIND GENeration program (WINDGEN) (Graber et al., 2006), produce wind analyses based on the assimilation of additional sources of data. However, they run independently and generate gridded wind fields that are not internally coupled to the storm surge prediction/wave models. Though not as sophisticated as finite-difference primitive-equation hurricane boundary layer wind models (Thompson and Cardone, 1996; Vickery et al., 2000), in the near field, when a hurricane approaches the shoreline and the storm's circulation dominates over the background synoptic flow, the NCFS wind formulation provides a remarkably realistic representation of the wind field at a fraction of the computational cost. It should be noted that the accuracy of the parametric wind fields strongly depends on the quality of the forecast guidance data provided by NHC.

The formulation of the asymmetric wind vortex is based on Xie et al. (2006):

$$P(r, \theta) = P_c + (P_n - P_c)e^{-[R_{\max}(\theta)/r]^B}, \quad (1)$$

where the surface pressure P varies as a function of the radial distance r from the hurricane center and the azimuthal angle θ around the storm, P_c is the central surface pressure of the storm, P_n is the ambient undisturbed synoptic background surface pressure, and R_{\max} is the radius of maximum wind, which varies azimuthally around the storm.

The tangential velocity V_{asym} is derived from the pressure field, assuming the winds are in gradient wind balance. In this case, the tangential acceleration vanishes and the flow is parallel to the isobars. The equation that describes a three-way balance between the radial pressure gradient, centrifugal and Coriolis forces can be inverted and solved to obtain the tangential wind velocity:

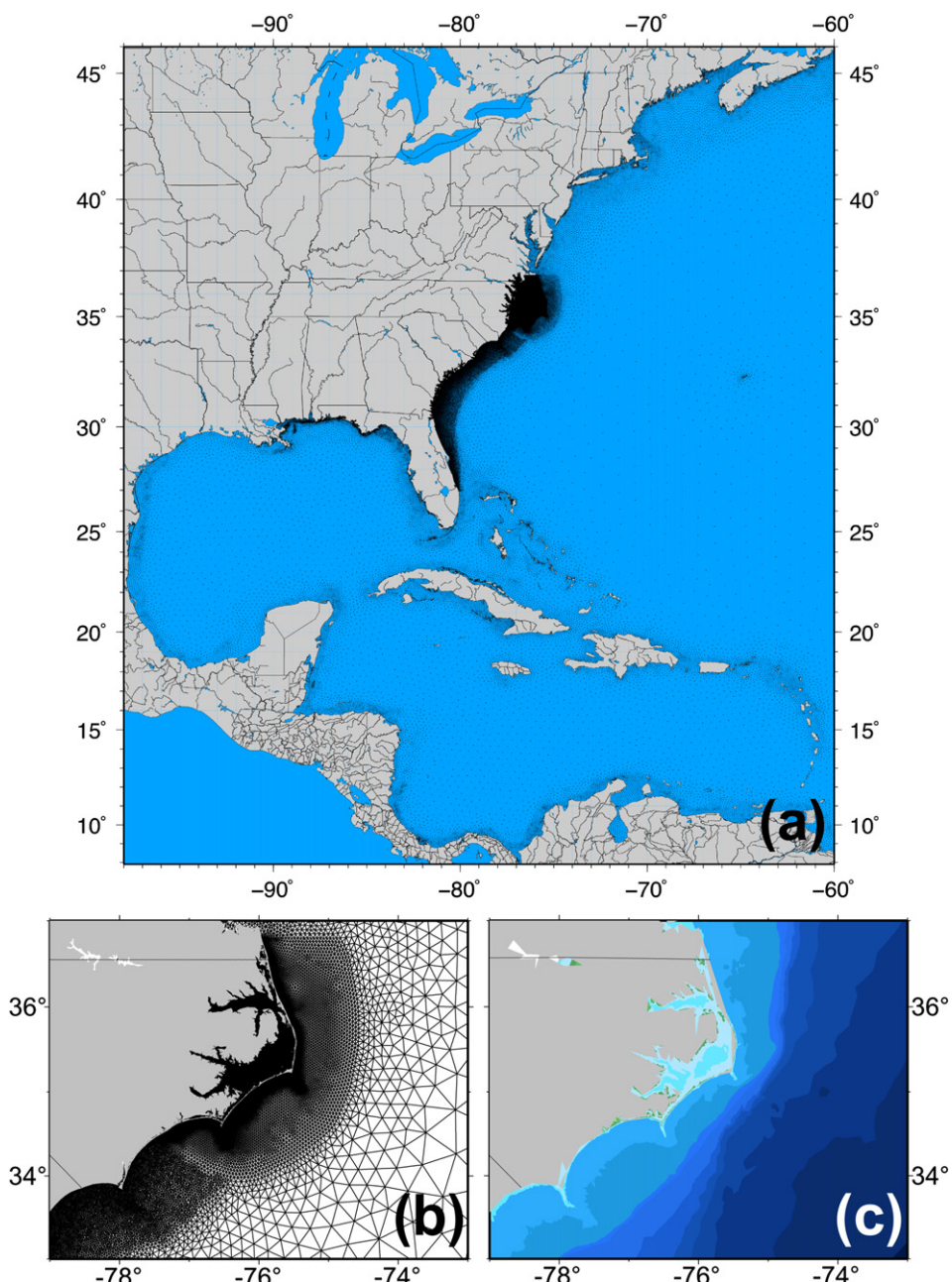


Fig. 1. (a) Model grid domain, (b) high-resolution NC grid and (c) bathymetry used in the NCFS version of the ADCIRC coastal ocean storm surge prediction model.

$$V_{\text{asym}} = \sqrt{\frac{B}{\rho_a} \left(\frac{R_{\max}(\theta)}{r} \right)^B (P_n - P_c) e^{-[R_{\max}(\theta)/r]^B} + \left(\frac{\eta f}{2} \right)^2 - \left(\frac{\eta f}{2} \right)}, \quad (2)$$

where ρ_a is the density of air, f is the horizontally varying Coriolis force, $f = 2\Omega \sin(\text{latitude})$ and Ω is the rotational frequency of the earth. The hurricane shape parameter B , which controls the eye diameter and steepness of the tangential velocity gradient, is computed from Eq. (2) using data from the NHC guidance at the radius of maximum winds:

$$B = \frac{[(V_{\max} - V_T)/W_{\text{PBL}}]^2 \rho_a e}{P_n - P_c}, \quad (3)$$

where V_{\max} is the maximum sustained (1 min) wind speed in the hurricane, V_T is the storm's forward motion, a translational storm velocity computed from successive NHC eye fixes that gradually ramps down to zero far from the storm's center, and W_{PBL} is a wind reduction factor, defined at the gradient wind flow level above the influence of the planetary boundary layer (Powell et al., 2003), used to adjust the wind speeds down to the surface. To limit the allowed shape and size of the vortex, B is restricted to values between 1 and 2.5.

This formulation was enhanced with a more precise radius of maximum winds root-finding algorithm based on Brent's method, and a cross-isobar frictional inflow angle of approximately 25° that decreases towards the center of the storm, as described in the Queensland Government's Ocean Hazards Assessment (2001):

$$\alpha_F = \begin{cases} 10 \frac{r}{R_{\max}}, & 0 \leq r < R_{\max}, \\ 10 + 75 \left(\frac{r}{R_{\max}} - 1 \right), & R_{\max} \leq r < 1.2R_{\max}, \\ 25, & r > 1.2R_{\max}. \end{cases} \quad (4)$$

In addition, the fourth-order polynomial curve fit for the radius of maximum winds vs. azimuth angle relationship used by Xie et al. (2006) was replaced with a cubic splines under tension fit, because the former introduced a numerical discontinuity at 0° and 360° due to the accumulation of error at the endpoints of the curve, a well-known artifact of least-squares polynomial curve fits. An added benefit of the new approach is an enhancement in the asymmetry of the vortex, making its shape more consistent with the observed/forecast wind radii reported by the National Hurricane

Center. The $R_{\max}(\theta)$ relationship is computed from the wind radii reported in the NHC forecast advisory at the highest closed isotach available.

A comparison of the winds produced by the symmetric and asymmetric Holland gradient wind vortex algorithms for Hurricane Ophelia (2005) is displayed in Fig. 2a and b. The asymmetry shifts the eyewall offshore, elongates the isotachs in the right front quadrant (RFQ) of the storm, and spreads the high winds northward along the Outer Banks.

Because the gradient wind relationship is strictly valid only at the top of the surface boundary layer, where the atmospheric flow decouples from surface friction (Powell et al., 2003), the winds are linearly extrapolated to the top of the mean boundary layer (MBL) by dividing by the aforementioned wind reduction factor W_{PBL} after subtracting the translational velocity V_T from the NHC advisory data. Once the shape parameter is calculated and the asymmetric R_{\max} vs. θ curve fit is performed, the tangential velocity V_{asym} can be computed from Eq. (2). The winds are calculated exactly at ADCIRC model finite-element nodal points, reduced back down to the surface, a 1-min to 10-min wind averaging operator is applied, the translational velocity components are restored, and the wind direction is deflected by the frictional inflow angle. This technique provides an analytical representation of a fully developed asymmetric tropical storm based on the following time-varying input parameters:

- (1) Surface pressure (mb) at the center of the storm: P_c .
- (2) Ambient undisturbed synoptic background surface pressure (mb): P_n .
- (3) Latitude (°N) and longitude (°E) of storm center: $cLat$, $cLon$.
- (4) Maximum sustained wind speed (knots) in the hurricane: V_{\max} .
- (5) Wind radii (nm) in four (NE, SE, SW, NW) quadrants of the storm at either 34, 50, 64, or 100 knots: $r(1)$, $r(2)$, $r(3)$, $r(4)$.
- (6) Wind speed (knots) at which the above wind radii are measured or forecast: V_r .
- (7) Date and time of the storm fix – used in computing the translational velocity (forward motion): year (yyyy), month (mm), day (dd), hour (hh).

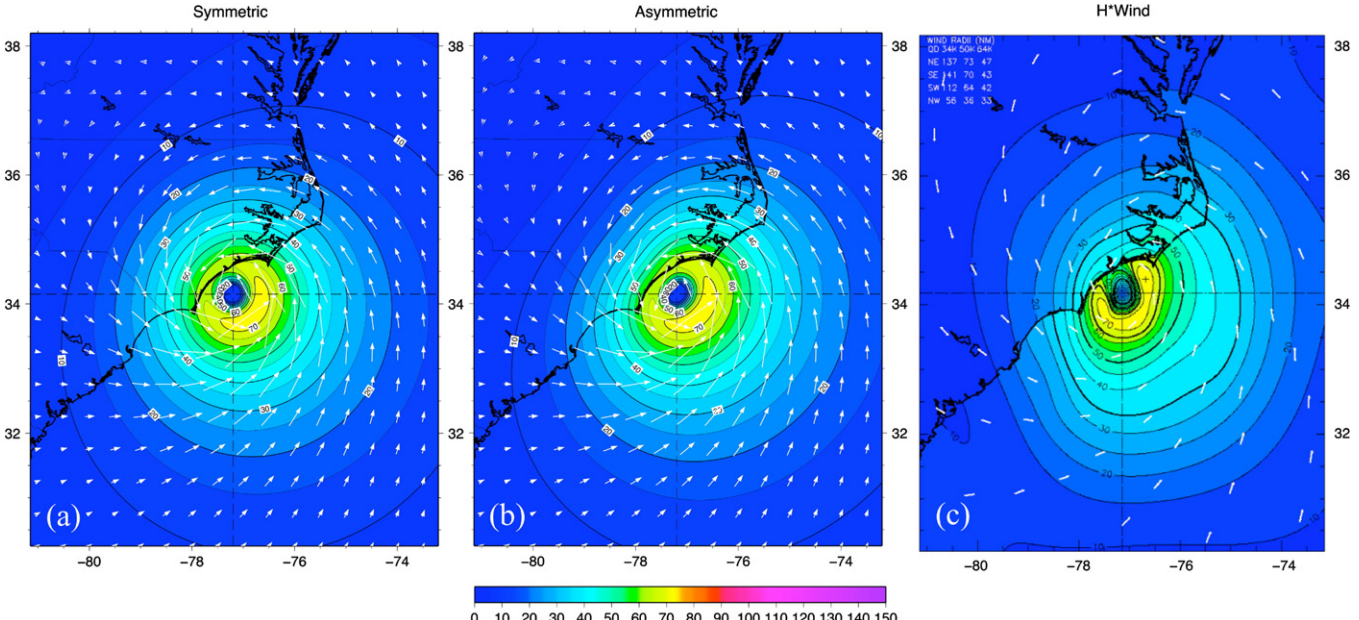


Fig. 2. Comparison of the winds produced by the (a) symmetric and (b) asymmetric Holland gradient wind vortex algorithm and (c) H*Wind analysis, all valid for Hurricane Ophelia at 22:30 UTC on September 14, 2005.

Winds generated using the asymmetric gradient wind vortex algorithm from both operational NHC forecast advisories and the Automated Tropical Cyclone Forecasting (ATCF) system corrected “best track” data for several historical storms were compared with the National Oceanic and Atmospheric Administration (NOAA) Atlantic Oceanographic and Meteorological Laboratory (AOML) Hurricane Research Division’s H*Wind surface wind analysis (Powell et al., 1998). Originally developed for input to DHS-FEMA’s HAZUS model, H*Wind analyses are generally considered to be the best wind estimates available. Measurements from a multitude of observational platforms are assimilated by the system, including NHC advisories, Automated Surface Observing System (ASOS) weather stations, NOAA buoy, Coastal Marine Automated Network (C-MAN) towers, ship reports, surface-reduced flight track measurements and GPS drop-windsondes from the NOAA P3, G4 and US Air Force C-130 reconnaissance aircraft, remotely sensed winds from the SSM/I

microwave radiometer, the ERS and QuikScat scatterometers, and the TRMM microwave imager onboard polar orbiting satellites, and GOES cloud drift winds derived from tracking low-level near-infrared cloud imagery in the geostationary satellite imagery. These winds are quality controlled, corrected for site exposure (marine or open terrain) and averaging period (maximum sustained 1-min wind speed), reduced to a height of 10 m, then composited relative to the storm over 4–6 h (Powell et al., 2004).

A comparison of the H*Wind and synthetic vortex winds is shown in Fig. 2b and c. The quality of the parametric rendition in Fig. 2b is remarkable, given that the asymmetric vortex was constructed from very little observed meteorological data (at the storm center and at four points in the surrounding quadrants) while the H*Wind analyses are constructed from a plethora of surface wind measurements. A banana-shaped swath of high velocity winds above 70 kt (36 m/s) is present on the right

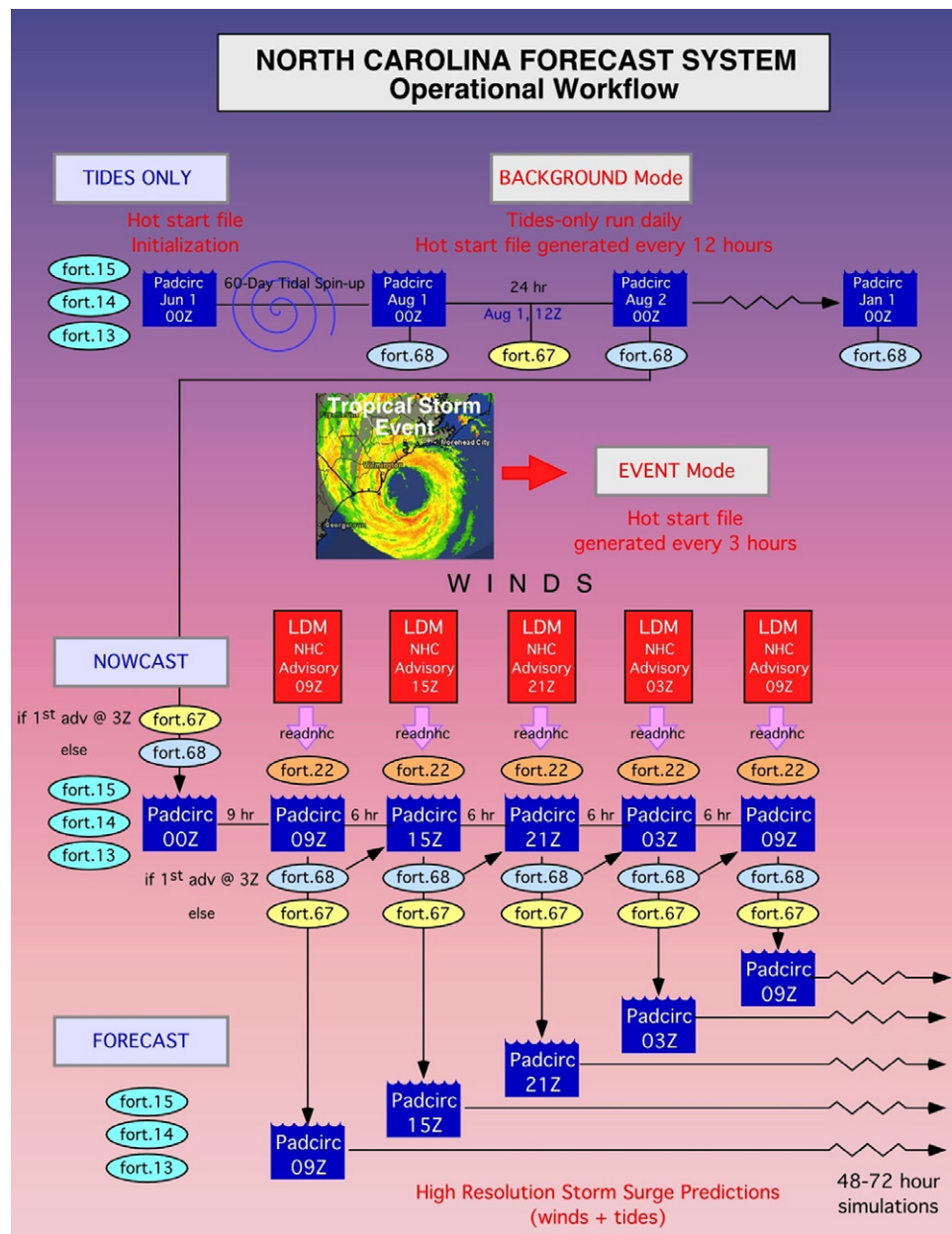


Fig. 3. Schematic depiction of the NCFS operational workflow for the 2006 hurricane season, showing its three different modes of operation.

side of the storm in Fig. 2b and the 65 kt (33.4 m/s) isotach wraps around three of the four quadrants, impinging on the shoreline in a very realistic manner. The frictional inflow angles are also well replicated, except far inland northwest of the storm. The greatest difference between the two wind representations is due to the use of an open-terrain exposure wind speed reduction algorithm over land in the H*Wind product, evident by the breaks in the isotachs at the coastline in Fig. 2c. Nevertheless, the aforementioned advantages of the analytical formulation and the timeliness in which the winds can be produced give the synthetic vortex approach an operational edge for the rapid prediction of storm surge.

3. The North Carolina forecast system operational workflow

A schematic depiction of the NCFS operational workflow is shown in Fig. 3. This logic was coded into Unix shell scripts for operational deployment.

The system runs in three modes: background (tides only), event nowcast (current state) and event forecast (future state).

3.1. Background mode: tides-only runs

Tides were included in all operational ADCIRC model simulations to obtain more accurate forecasts of storm surge along the NC coastline. Although the total tide is composed of approximately 399 known tidal constituents (Doodson, 1922), most have very small amplitudes. Only the largest eight are required to capture 90% of the tidal signal for ocean modeling applications. Therefore, the eight primary lunar and solar tidal harmonic constituents (M_2 , S_2 , K_2 , N_2 , K_1 , O_1 , P_1 , Q_1) were prescribed at the open water boundaries and applied as tidal potential constituents in the interior of the ocean model domain.

Two steps are needed to incorporate the tides into ADCIRC. The first is the extraction of tidal data from a tidal database. The open-water lateral boundary conditions and tidal potential terms for the high-resolution NC ADCIRC model are generated from Oregon State University's TPXO Topex/Poseidon global model of ocean tides (<http://www.oce.orst.edu/research/po/research/tide/global.html>). The second step is to convert the data into ADCIRC format so it can be included in the input file.

The start date for the initialization of the operational system was 0:00 UTC June 1, 2006. The harmonic constituents used, their nodal factors, and equilibrium arguments are shown in Table 1. These two parameters are essential for “starting the clock” in an ADCIRC simulation and provide proper time synchronization for direct comparison with observations. The hot start (restart or checkpoint) files are kept up-to-calendar-date (“dragged along”) by running tidal simulations every 24 h. The hot start files are saved every 12 h.

Table 1

Harmonic constituents, their nodal factors and equilibrium arguments used in the NCFS

Harmonic constituent	Nodal factor	Equilibrium argument (deg)
M_2	0.963170	250.63
S_2	1.000000	0.00
N_2	0.963170	110.92
K_2	1.317220	138.86
K_1	1.112810	159.43
O_1	1.183150	91.17
P_1	1.000000	200.66
Q_1	1.183150	311.46

3.2. Event nowcast mode

The NHC forecast advisories are issued every 6 h at 3:00 UTC, 9:00 UTC, 15:00 UTC and 21:00 UTC. The NHC forecast advisory data are broadcast directly through the LDM in real time. These forecast advisories are fed to the LDM within 1–2 min after the Hurricane Specialists at NHC/TPC “hit the button” that submits the forecast to the National Weather Service (NWS) telecommunications gateway. Sent through AWIPS, then placed on the NOAA-PORT, they are transmitted through the high-bandwidth Family of Services (FOS) Domestic Data Plus (DD+) stream to subscribed LDMs. In order to capture this data, a line containing a regular expression was inserted into the LDM's pqact configuration-file (pqact.conf_ddplus) to detect the AWIPS headers (MIATC-MAT1-5) and the World Meteorological Organization (WMO) headers (WTNT21–25 KNHC) that identify these products. As soon as they enter the data stream, the LDM PIPE command is used to automatically start up a Unix shell script (invokeStorm-Surge.sh) that preprocesses this data and initiates the model run.

A NHC forecast advisory parser/decoding Fortran program was developed to extract the current and forecast hurricane winds and radii information, then rewrite this data in compact “best track” format to very small output files to run the nowcast and forecast modes. A new acronym (ASYM) for the four-letter objective technique designator was created to tag the records produced in this manner. These files are used to construct the synthetic asymmetric wind vortex that drives the ADCIRC model during the nowcast and forecast simulations.

Once a tropical storm enters the ADCIRC model domain (west of 60°W and north of 7.9°N), far in advance of an event that would threaten the NC coastline, nowcast mode is automatically switched on. The nowcast runs bring the initial conditions up-to-date.

The first storm surge nowcast simulation starts with the most recent tides-only hot start file and uses the wind information from the first NHC forecast advisory to update the model to the current state. For the first advisory, the tides from the previous day at 12:00 UTC are used for a 3:00 UTC initialization while the tides at 0:00 UTC that same day are used to initialize simulations from the 9:00 UTC, 15:00 UTC and 21:00 UTC advisories. This ensures that the model spin-up time for the first advisory is at least 9 h in duration, which allows any spurious transient waves generated by initialization shock to dissipate. The results are saved to initialize the nowcast phase of the next storm advisory run and the current forecast simulation.

From the first advisory on, successive advisories arrive 6 h apart. For subsequent advisories, the system uses the previous nowcast results and the current advisory data to update the model elevations.

3.3. Event forecast mode

After each nowcast is completed, a second model run, initialized with the forecast data from the NHC forecast advisories, is triggered. These forecast simulations generate a series of 48–72 h storm surge forecasts. From the time a NHC forecast advisory is issued until the time a product (horizontal plot of surge, current velocity, wind, etc.) is displayed on a web site requires about one hour when integrating ADCIRC with a time step of 1 s and running on 128 processors on the Renaissance Computing Institute's (RENCI's) 4096-processor IBM Blue Gene/L system or the University of North Carolina's 4160-processor Linux 2.3 GHz Intel Clovertown Topsail cluster (Mattocks et al., 2006; Forbes et al., 2008). The parametric asymmetric wind model, directly coupled to ADCIRC at every grid point and time step, is extremely computationally efficient. In the current NCFS configuration, it adds about 6.5 min of CPU time to a 3-day simulation, which is negligible when com-

pared with the hours required to wait, download, preprocess and interpolate gridded wind fields of inferior spatial resolution and temporal frequency.

The system's reliability is being continuously hardened. Its fault tolerance and recovery have been enhanced through the incorporation of new error checks in the model source code and operational shell scripts that detect whether a storm is inside the ADCIRC grid domain, switch the workflow logic to respond to the issuance of special advisories by NHC, adjust the parametric wind model to compensate for missing wind radii, etc. Although a backup FTP capability has been developed, there has not yet been a need to activate it because the LDM has proven to be extremely reliable in delivering the small packets of initialization/forecast information that the NCFS requires.

4. Operational storm surge predictions

A late-breaking El Niño ocean surface warming event in the equatorial Pacific induced vertical wind shear in the Caribbean basin that suppressed hurricane formation, thus no hurricanes hit the US coastline during the 2006 season. Nevertheless, NCFS storm surge predictions were produced in real time for several tropical storms. Results from simulations of Tropical Storm (TS) Ernesto are presented since it had the most impact on North Carolina.

TS Ernesto developed in a dry, sheared environment from a tropical wave that moved through the windward islands on August 24, 2006. Originally forecast to track through the Caribbean and into the Gulf of Mexico, it turned northward instead, survived being ripped apart by the mountainous terrain in eastern Cuba, then crossed through the heart of the Florida peninsula from the south. A tenacious storm, it re-emerged over the Atlantic Ocean near Cape Canaveral late in the day on August 30. NCEP's NAM model persistently forecast Ernesto to be absorbed by a frontal system inland over South Carolina (SC) and dissipate but it remained offshore, intensified and just missed becoming a Category 1 hurricane, with its peak winds nearing 75 mph, prior to making landfall at Oak Island, NC, a few miles south-southwest of Wrightsville Beach, around 11:40 p.m. Thursday, August 31, 2006 (3:40 UTC, September 1, 2006).

Fig. 4a shows the actual track (red) of TS Ernesto superimposed with NHC's operational 6-h forecast track (brown) and 12-h forecast track (green). The predicted landfall location shifted eastward by approximately 100 miles (161 km) in 12 h, from the Myrtle Beach area in South Carolina to the Holden Beach-Southport area along the southern coast of North Carolina. This error in the 12-h forecast track is well beyond 35.3 nautical miles (63.4 km), the value used to define the radius in NHC's cone of uncertainty (http://www.nhc.noaa.gov/verification/pdfs/OFCL_5-yr_averages.pdf). Sudden changes like these in the predicted landfall location of tropical cyclones are good tests of an operational forecast system and justify the choices made in the design of the NCFS. If the TS Ernesto storm surge predictions had been delayed 3–6 h while waiting to download and process the NCEP NAM model wind and pressure fields, there would have been very few hours of forecast utility remaining.

The NOAA/NOS/CO-OPS sea surface elevation record for the station at Wrightsville Beach is displayed in Fig. 4b. It shows that TS Ernesto created a maximum surface elevation of 1.22 m (4.00 ft) at 3:42 UTC and a surge above tides of 0.98 m (3.22 ft).

4.1. Event forecast mode

The 10-min averaged synthetic asymmetric vortex winds generated from NHC's 12-h forecast advisory, valid at 3:00 UTC on September 1, 2006, are shown in Fig. 5a. Note that the predicted

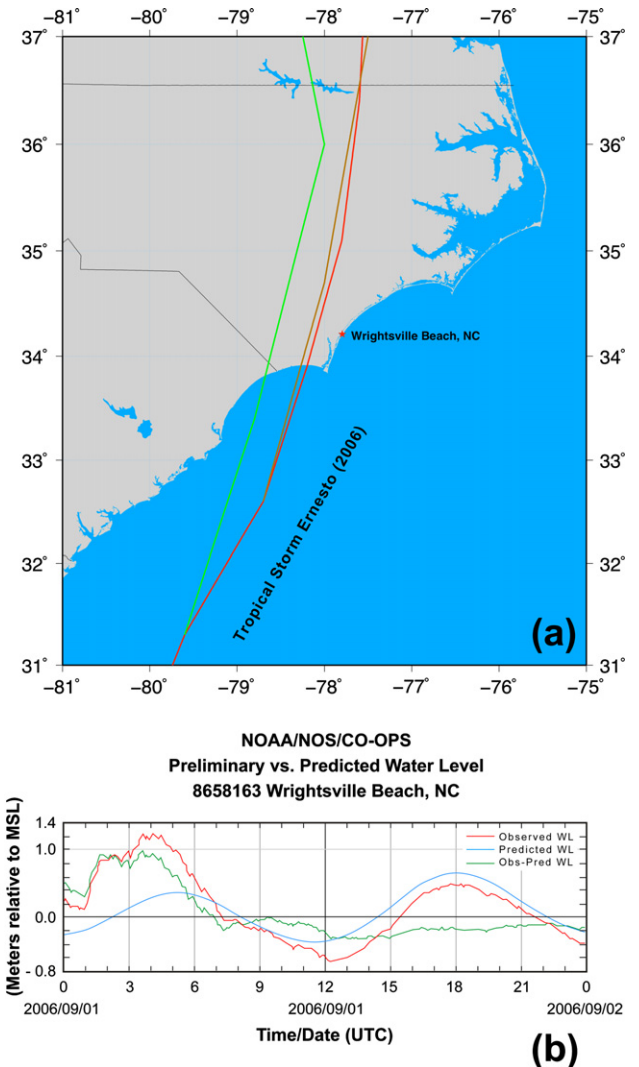


Fig. 4. (a) Official National Hurricane Center "best track" (red) of Tropical Storm Ernesto superimposed with the operational 12-h (green) and 6-h (brown) forecast tracks. Note the abrupt shift eastward in the predicted landfall location over 12 h. (b) Recorded sea surface elevation for the NOAA/NOS/CO-OPS station at Wrightsville Beach, NC.

center of TS Ernesto is located in South Carolina very close to the SC-NC border. Winds of 26.6 m/s (51.8 kt) are predicted in the Wilmington area. The predicted sea surface height and currents for the 12-h forecast run are displayed in Fig. 5d. A maximum water surface elevation of 1.60 m (5.23 ft) is predicted up the Cape Fear River. The currents flow primarily northeastward, parallel to the NC coastline north of the SC-NC border, while there is a strong offshore component southwest of the hurricane. The storm surge above tides, calculated by removing the model-predicted tides from the simulated sea surface elevation, is displayed in Fig. 5g. A maximum surge above tides of 1.72 m (5.64 ft) is predicted in the Cape Fear River.

The 10-min averaged synthetic asymmetric vortex winds generated from NHC's 6-h forecast advisory, valid at 3:00 UTC on September 1, 2006, are shown in Fig. 5b. The center of the storm has moved eastward along the coast and is now located in the Holden Beach area along the southern coast of North Carolina. The highest predicted wind speeds have shifted offshore and their intensity has increased to 28 m/s (54.5 kt). The predicted sea surface height and currents for the 6-h forecast run are displayed in Fig. 5e. The large-scale sea surface height maximum

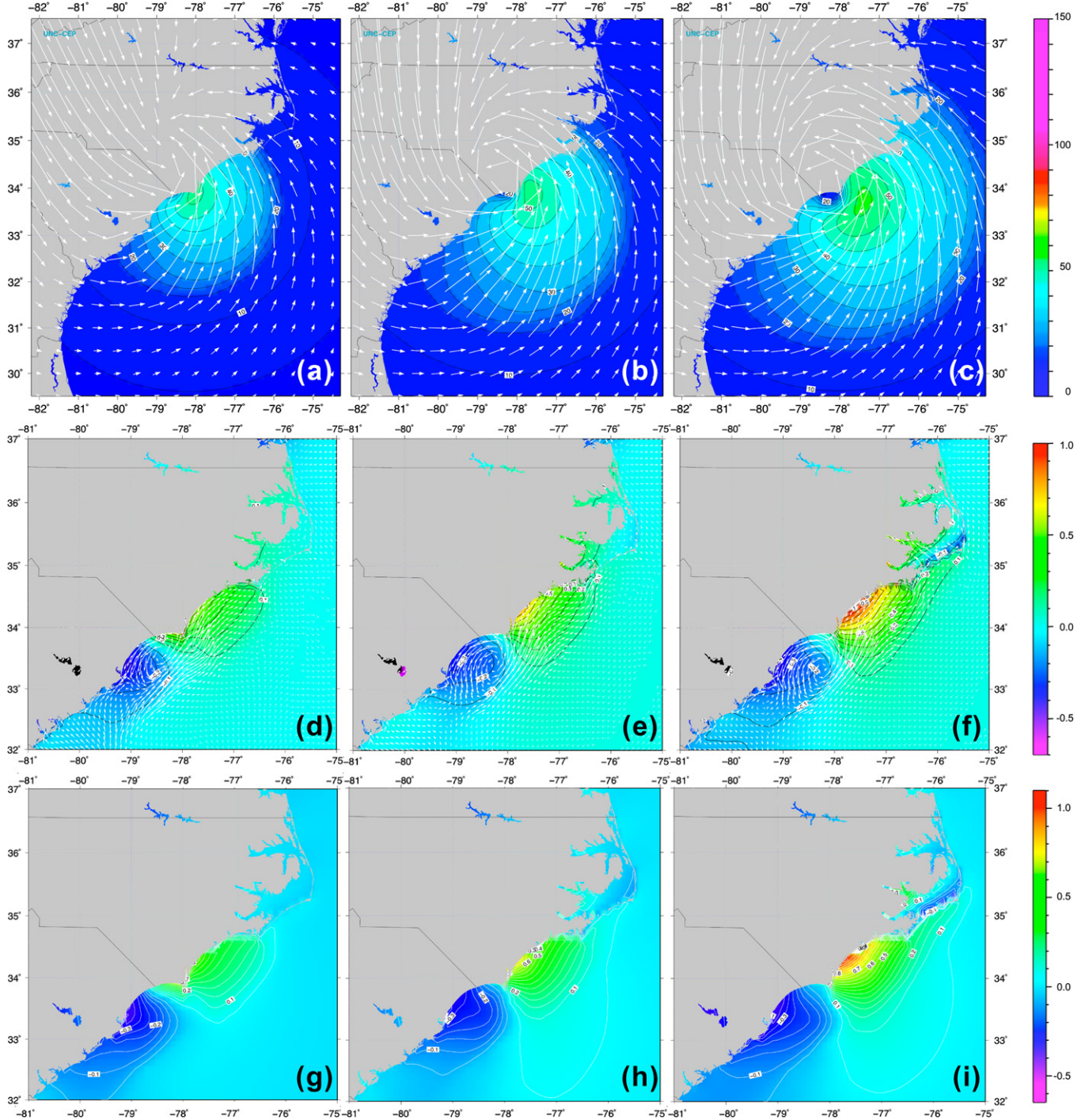


Fig. 5. 10-Min averaged synthetic winds (kt) generated from NHC's (a) 12-h forecast advisory, (b) 6-h forecast advisory and (c) 0-h analysis. Predicted sea surface elevation (m) and currents (m/s) from (d) a 12-h forecast, (e) a 6-h forecast and (f) a 0-h (nowcast). Predicted storm surge (m) above tides from (g) a 12-h, (h) a 6-h forecast and (i) 0-h (nowcast). All panels are valid for TS Ernesto at 3:00 UTC on September 1, 2006.

has moved up the coast and increased in magnitude. The surge up the Cape Fear River, about 0.90 m (2.95 ft), is smaller than in the 12-h forecast, even though the winds have intensified. This is because the currents are now more perpendicular to the coastline, across the river's mouth, instead of flowing up the river. The 6-h forecast predicts that the storm surge above tides (Fig. 5f) has diminished to 1.3 m (4.27 ft) with the maximum shifted further east along the coast than in the 12-h forecast.

4.2. Event nowcast mode

The 10-min averaged synthetic asymmetric vortex winds from the nowcast simulation, valid at 3:00 UTC on September 1, 2006, are displayed in Fig. 5c. It shows the center of TS Ernesto close to landfall, which officially occurred 40 min later. The sea surface heights that were generated from an ADCIRC simulation driven by these winds are displayed in Fig. 5f. The sea surface elevation is greater than 1 m in a swath near Topsail Beach along the south-

eastern coast of NC. There are some small isolated peaks of high surface elevation further to the northeast and a sound-side maximum of 1.48 m (4.86 ft) close to Emerald Isle, NC. Also evident in Fig. 5f is a large gradient across Pamlico Sound, high elevations up the Neuse River, and strong currents in the Croatan Sound and Alligator River. The storm surge above tides for the nowcast simulation is shown in Fig. 5i. The maximum at 3:00 UTC was 1.15 m (3.77 ft), lower than in the previous ADCIRC forecasts. However, higher surface elevations are distributed more broadly over a larger area along the NC coast, instead of occurring at isolated locations.

The sea surface heights from the ADCIRC 12-, 6- and 0-h forecasts (the latter defined as the nowcast) are compared with the NOAA/NOS-CO-OPS observations at Wrightsville Beach, NC in Fig. 6.

It displays the evolution of the sea surface elevations with decreasing forecast lead time. As expected, the simulated sea surface height approaches the observations as the forecast times approach the time of the storm's landfall. The maximum sea surface height in the 12-, 6-, and 0-h forecasts is 0.57 m (1.87 ft),

0.74 m (2.43 ft), and 0.99 m (3.25 ft), respectively, while the highest elevation observed at Wrightsville Beach is 1.22 m (4.00 ft), which occurs slightly after the maximum predicted by the model. This occurs because the next forecast advisory at 9:00 UTC did not contain any wind radii information, so the winds from the previous advisory were used to force the storm surge prediction model. The difference between the 12-h forecast and the nowcast is 0.42 m (1.38 ft), while the difference between the 6-h forecast and the nowcast is only 0.25 m (0.82 ft).

4.3. Hindcasts

In order to quantify the results obtained from the operational predictions run during the 2006 hurricane season, two cases were run retrospectively with different types of wind forcing. In the first case, the real-time NCFS forecasts were compared with simulations driven by NHC's official best track wind information (in "best track hindcast" mode) to evaluate how errors in NHC's track/intensity forecasts impact the quality of the storm surge predictions. In the second case, the model was driven with winds from H*Wind analyses to

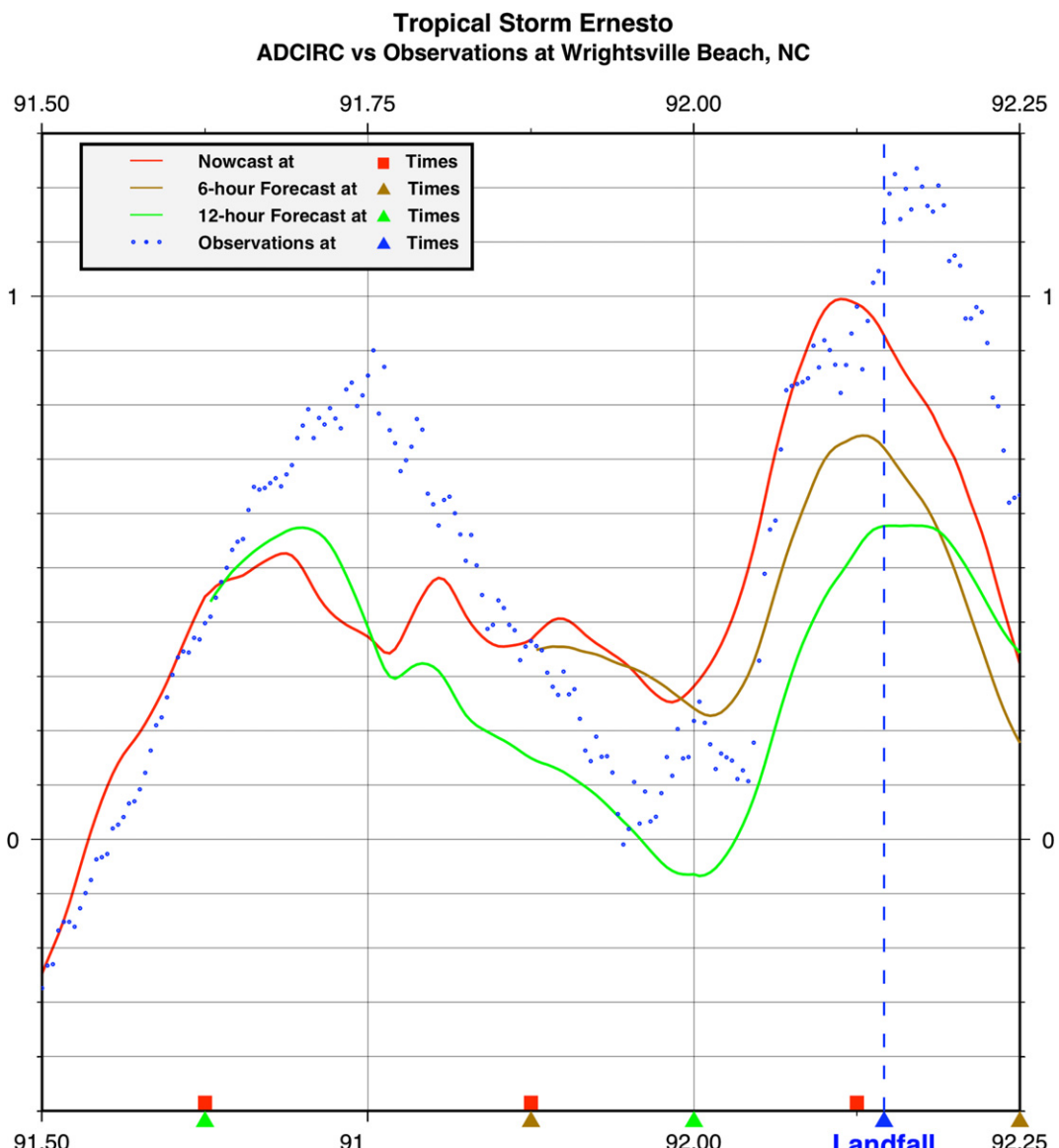


Fig. 6. Evolution of the sea surface elevations (m) predicted from a 12-h ADCIRC forecast (green), 6-h forecast (brown), and nowcast (red) simulations of TS Ernesto vs. NOAA/NOS-CO-OPS observations (blue dots) at Wrightsville Beach, NC.

determine how well the synthetic asymmetric vortex winds forcing compares with forcing from a complete, data-rich wind field.

4.3.1. Best track

The synthetic winds derived from the best track data at 3:00 UTC September 1 are shown in Fig. 7a.

These winds are slightly lower than the synthetic winds produced from the real-time NHC forecast advisories (Fig. 5c). The areal extent of the 45 kt (23.1 m/s) isotach is reduced and the overall width of the storm is smaller. On the other hand, the eye diameter is larger in the best track rendition. The best track storm center is further offshore than the storm constructed from the operational NHC advisory winds.

The sea surface height and currents from the simulation forced with the best track winds are displayed in Fig. 7b. The sea surface height maximum in the right front quadrant of the storm and the drawdown on the west side of the storm are both reduced in magnitude. However, higher elevations occur in the Pamlico Sound to the lee of the barrier islands, while lower elevations occur along the coast and up the Neuse River in the simulation driven by best track winds, when compared against the case forced with real-time NHC advisory data. The storm surge along the coast produced by the best track winds forcing (Fig. 7c) is much smaller in magnitude than in the asymmetric NHC winds case (Fig. 5i) and it is not so widely spread offshore.

4.3.2. H*Winds

Fig. 7d shows the ADCIRC winds generated from the H*Winds analysis for September 1 at 3:00 UTC. The storm is less intense but has the same general distribution of winds. The maximum wind intensity is 52.2 kt (26.8 m/s), compared to the NHC advisory-derived winds of 56.1 kt (28.9 m/s). Note, in Fig. 7e, that the sea surface height is also smaller in the H*Winds driven storm surge simulation, with a maximum of 0.92 m (3.02 ft). The sea surface height gradients in Pamlico Sound exhibit a different distribution due to a more easterly wind direction and the drawdown to the west of the storm is smaller in magnitude, consistent with the increased wind drag over land and the lower winds blowing offshore in that area. The maximum storm surge above tides generated by the H*Winds driven simulation, shown in Fig. 7f, is 0.80 m (2.62 ft), the smallest value obtained in all the simulations for this particular time.

4.4. Comparison with NOAA observations

ADCIRC has the capability to interpolate surface elevation, current velocity, wind and atmospheric pressure from its finite-element grid nodes to user-specified station locations or any other locations of interest. This feature is particularly useful for validating simulation results.

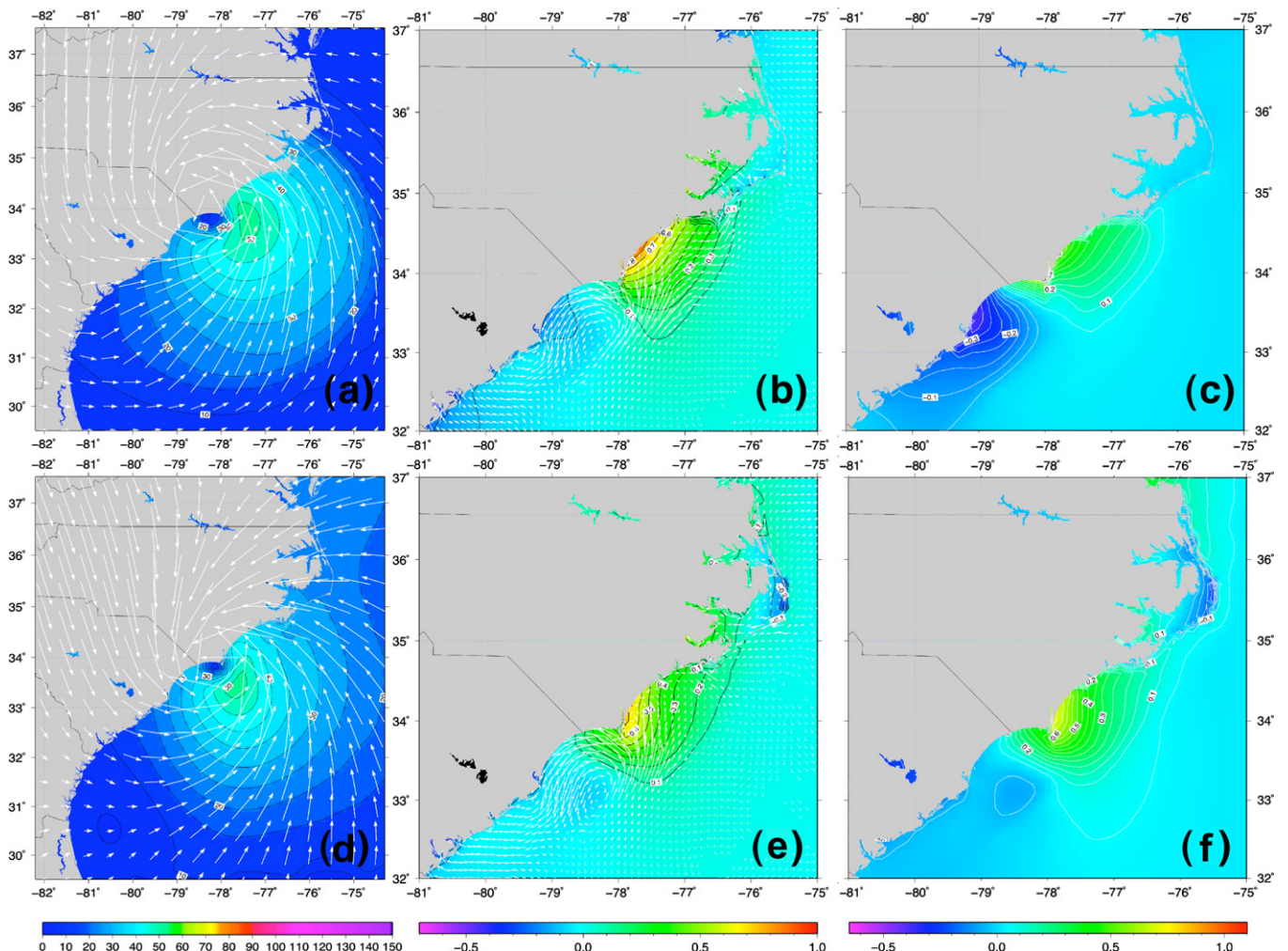


Fig. 7. (a) 10-Minute averaged synthetic winds (kt) generated from the best track data, (b) sea surface elevation (m) and currents (m/s) forced with best track winds, (c) simulated storm surge (m) above tides forced with best track winds, (d) ADCIRC winds (kt) generated by H*Winds analysis, (e) sea surface elevation (m) and currents (m/s) from ADCIRC simulation forced with H*Winds, and (f) simulated storm surge (m) above tides forced with H*Winds. All panels are valid for TS Ernesto at 3:00 UTC on September 1, 2006.

The model results were compared to the actual observations at several stations along the NC coast from simulation day 88 to 92,375, which correspond to the calendar period of 0:00 UTC August 28, to 9:00 UTC September 1, 2006. Fig. 8a shows the ADCIRC model tides compared with the NOAA predicted tides at Wrightsville Beach, NC. There is an offset of about 10 cm (3.9 in) between the two. This is important to point out since the ADCIRC surface elevation could be adjusted by this amount to calibrate the model's storm surge predictions in the future or the grid resolution could be further refined. For comparison purposes, this offset can be removed by subtracting the running time-mean from each of the sea surface elevation traces.

Fig. 8b shows a comparison between the actual NOAA tidal station observations and the ADCIRC model elevations produced by simulations driven by different wind forcing: (1) best track dataset, (2) NHC advisories and (3) H*Winds. The time period when TS Ernesto was closest to the NC coast (grey square in Fig. 8b) was further analyzed. The surge above tides was calculated by removing the model tides from the model elevations, and the NOAA predicted tides from the NOAA observed elevations (Fig. 8c). The maximum sea surface elevation produced by the model simulation forced with NHC advisory winds was 0.99 m (3.25 ft) at Wrightsville Beach and the surge above tides was 1.06 m (3.48 ft) vs. the observed sea surface elevation of 1.22 m (4.00 ft) and surge of 0.98 m (3.22 ft), a difference in the surge of only 8 cm (3.15 in) or 8%. The maximum predicted surge occurs somewhat earlier than the observations when the tides are slightly lower. The predicted storm surge agrees well with the 0.91–1.52 m (3–5 ft) range that was predicted by NHC and observed. The red triangles at the bottom of the graph show the times when the NHC forecast advisories were issued and automatically kicked off an operational ADCIRC model run. The brown triangles show the times at which the corrected best track data are available.

In general, at the time when an NHC advisory was issued or best track data were available, the observations agree with the model results. The simulations in which the NHC advisories are in good agreement with the observations are initialized at 9:00 UTC and 3:00 UTC, and at 0:00 UTC for the best track, as pointed out earlier for the surface elevation. Since the storm made landfall at 3:40 UTC, then proceeded inland and slowly decayed, the data available from the advisories cannot reproduce the peak at 3:40 UTC. The best track forced simulation follows the signal produced by the ADCIRC simulation driven with the synthetic winds generated from NHC advisories. It is in even better agreement with the observations at the times that track fixes are available. The H*Winds forced simulation underpredicts the storm surge prior to landfall but performs best at landfall. Table 2 provides a summary of the simulated and observed maximum/minimum sea surface height and surge above tides at Wrightsville Beach.

After running numerous retrospective sensitivity tests on this storm, it was discovered that using a background pressure of 1009 mb (obtained from the best track data) for this case, instead of the operational default US Standard Atmosphere value of 1013 mb, improved the predicted sea surface elevation significantly, reducing the RMS error by 11%, and bringing it closer to the observations. Unfortunately, there is no information about the background pressure in the NHC forecast advisories, so a real-time source of this information (possibly a value distilled from an earlier NCEP atmospheric model forecast) will be sought in the future.

5. Additions to the ADCIRC model to increase its accuracy

Two important enhancements that had recently been implemented in the ADCIRC model were tested to assess the improvement in the accuracy of the NCFS storm surge predictions. The first is a directional surface roughness parameterization that mod-

ulates the wind speed at a given location, and applies forest canopy sheltering if appropriate, based on the types of land cover encountered upwind. The second enhancement is a spatially varying distribution of Manning's-n friction coefficient used for computing the bottom/channel bed friction.

Coastal land cover data from the 2001 National Land Cover Dataset (NLCD), which has a horizontal resolution of 30 m, was preprocessed to account for wind exposure in 30° wind direction increments and overwash during inundation events (Mattocks et al., 2006). The surface roughness length z_0 and the hydrologic Manning's-n friction coefficient for each land cover type were obtained from values published in earlier studies (see Arcement and Schneider, 1989 for a thorough review). A data table consisting of 29 land cover classes was created with class ID, class name, Manning's-n friction coefficient, surface roughness length, and forest canopy sheltering factor (Table 3).

5.1. Calculation of directional surface roughness length

Described in detail by Westerink et al. (2008), the algorithm for the wind drag induced by spatially varying land friction reduces hurricane winds to account for the higher surface roughness that exists over land. This gradual upwind modulation is consistent with the fact that the boundary layer does not adjust to a new roughness instantaneously. Simulating this effect is crucial in coastal regions because winds that transition from land to water would suddenly accelerate and be incorrectly simulated at full marine force in the nearshore zone without it, while marine winds that penetrate inland would suddenly "hit the wall", decelerate and be unrealistically diminished.

Nodal attribute arrays were built for surface roughness length values in 12 clockface positions for each model node in the ADCIRC grid domain. The directional roughness length value was computed based on the land cover types within a range of 10 km upwind. As per Westerink et al. (2008), a Gaussian weighting function was used to compute distance-based weights $w(i)$:

$$w(i) = \frac{1}{\sigma\sqrt{2\pi}} e^{-\left(\frac{d(i)^2}{2\sigma^2}\right)}, \quad (5)$$

where $d(i)$ is the distance between the ADCIRC model node and a land cover pixel, and σ is set to 3 km. As explained by Powell et al. (2005), the dynamical basis for this formulation is provided by reverse plume modeling studies that take into account the turbulence created by patchy terrain and determine the relative importance of the turbulence source area on a downstream wind sensor. The flow is most influenced by the fetch-dependent surface roughness 3 km upstream of the grid node centroid but the flow is still modulated by the terrain further upstream (up to 10 km away). The weighted land cover surface roughness length values are summed within each sector and normalized to obtain the upwind land surface roughness length coefficient $z_{0\text{land-directional}}$:

$$z_{0\text{land-directional}} = \frac{\sum_{i=0}^n w(i) z_{0\text{land}}(i)}{\sum_{i=0}^n w(i)}, \quad (6)$$

where i is the index of the pixel, n is the number of land cover pixels in a sector, and $z_{0\text{land}}(i)$ is the surface roughness length value at the pixel.

The spatial distribution of the surface roughness length and the impact of the directional upwind parameterization can be seen more clearly by examining an ADCIRC model node (#70717 located at 34.61°N, 76.54°W) that falls on Cape Lookout, NC (Fig. 9c), a cusplike coastline feature where there is a large variation in the surface characteristics (Fig. 9a) that can impact the winds depending on their direction.

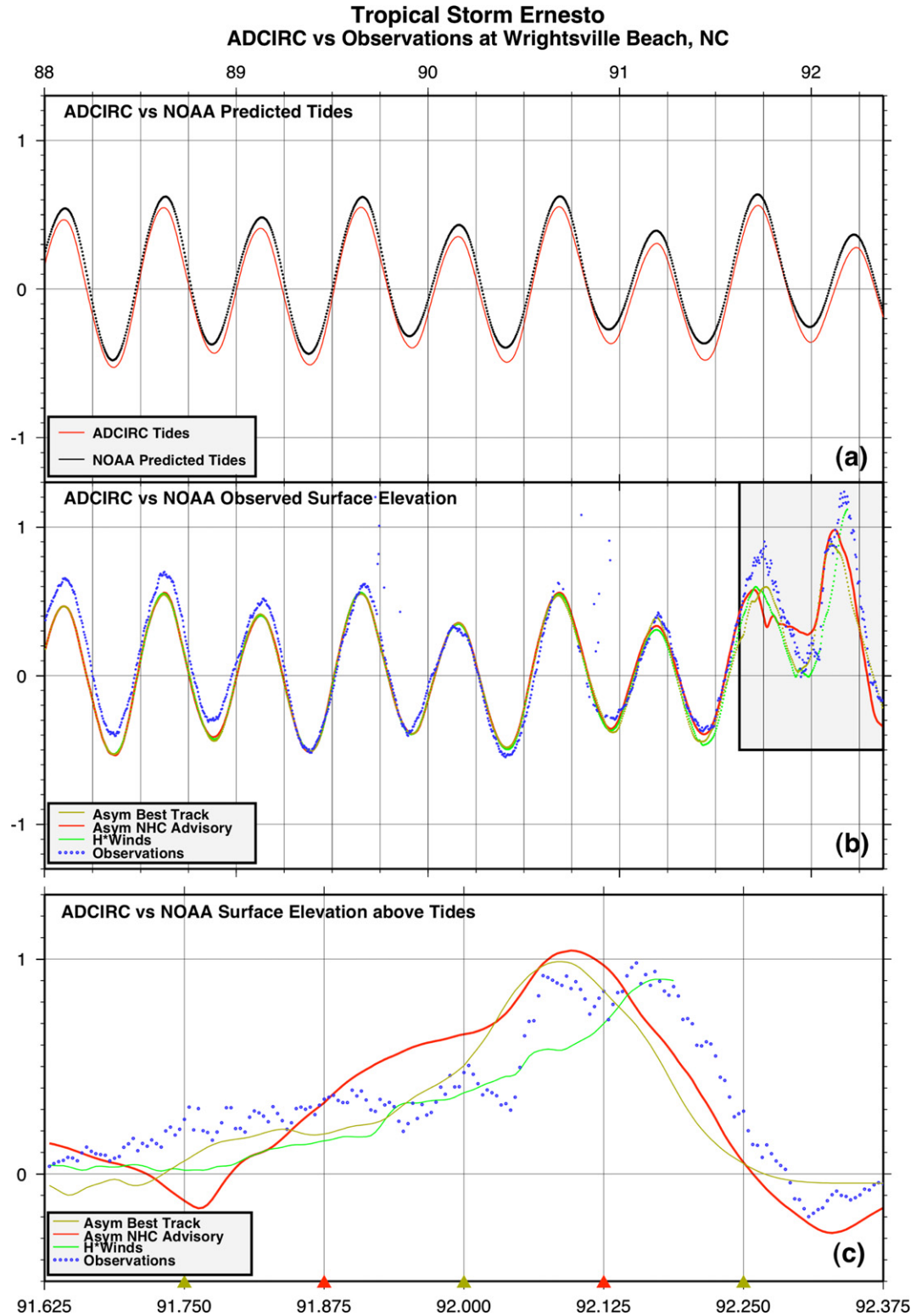


Fig. 8. ADCIRC model sea surface elevations (m) vs. NOAA/NOS/CO-OPS observations (m) at Wrightsville Beach, NC from simulation day 88 (August 28, 2006 at 0:00 UTC) until simulation day 92.375 (September 1, 2006 at 9:00 UTC). (a) ADCIRC model tides (m) vs. NOAA predicted tides (m), (b) NOAA tidal station observations (m) vs. ADCIRC model elevations (m), and (c) NOAA observed minus predicted surface elevation (m) and ADCIRC surge above tides (m) produced by simulations driven with best track data, NHC advisories, and H*Winds during the time frame depicted in the gray square in panel (b). The red triangles at the bottom of the graph show the times when the NHC forecast advisories were issued and automatically kicked off an operational ADCIRC model run. The brown triangles show the times at which the corrected best track data are available.

A polar coordinate “rose” plot of the values of the surface roughness length (m) as a function of wind direction at ADCIRC model node #70717 is displayed in Fig. 9b. The rose plot shows that the roughness is lowest for winds blowing from the south-

west over open water. The highest values occur when the winds traverse long stretches of developed or forested land within a 3 km radius of the node, such as in the northeast and southeast sectors.

Table 2

A summary of the maximum/minimum sea surface height and surge above tides (m) for the NOAA tidal station at Wrightsville Beach, NC (OBS), the corresponding model recording station for the various simulations performed: 12-h forecast (FOR-12), 6-h forecast (FOR-6), nowcast with NHC forecast advisory derived asymmetric winds (NOW-NHC), nowcast with asymmetric winds derived from the best track dataset (NOW-BTK), and H*Winds analyses (NOW-HW). Times are on Sept 1, 2006

Simulation	SSH max (m) Wrightsville	Surge above tides max (m) Wrightsville	Surge above tides time (UTC) Wrightsville
FOR-12	0.57	0.530	2:30
FOR-6	0.74	0.780	2:24
NOW-NHC	0.99	1.060	2:24
NOW-BTK	0.88	0.971	2:24
NOW-HW	1.12	0.906	4:12
OBS	1.22	0.982	3:42

Table 3

NLCD land cover classes with assigned values for the Manning's-n friction coefficient, surface roughness length and forest canopy sheltering factor (based on Mattocks et al., 2006)

NLCD class number	NLCD class name	Manning's-n friction coefficient	Surface roughness length (m)	Canopy
11	Open Water	0.020	0.001	1
12	Perennial Ice/Snow	0.010	0.012	1
21	Developed – Open Space	0.020	0.100	1
22	Developed – Low Intensity	0.050	0.300	1
23	Developed – Medium Intensity	0.100	0.400	1
24	Developed – High Intensity	0.150	0.550	1
31	Barren Land (Rock/Sand/Clay)	0.090	0.040	1
32	Unconsolidated Shore	0.040	0.090	1
41	Deciduous Forest	0.100	0.650	0
42	Evergreen Forest	0.110	0.720	0
43	Mixed Forest	0.100	0.710	0
51	Dwarf Scrub	0.040	0.100	1
52	Shrub/Scrub	0.050	0.120	1
71	Grassland/Herbaceous	0.034	0.040	1
72	Sedge/Herbaceous	0.030	0.030	1
73	Lichens	0.027	0.025	1
74	Moss	0.025	0.020	1
81	Pasture/Hay	0.033	0.060	1
82	Cultivated Crops	0.037	0.060	1
90	Woody Wetlands	0.100	0.550	0
91	Palustrine Forested Wetland	0.100	0.550	0
92	Palustrine Scrub/Shrub Wetland	0.048	0.120	0
93	Estuarine Forested Wetland	0.100	0.550	0
94	Estuarine Scrub/Shrub Wetland	0.048	0.120	1
95	Emergent Herbaceous Wetlands	0.045	0.110	1
96	Palustrine Emergent Wetland (Persistent)	0.045	0.110	1
97	Estuarine Emergent Wetland	0.045	0.110	1
98	Palustrine Aquatic Bed	0.015	0.030	1
99	Estuarine Aquatic Bed	0.015	0.030	1

Fig. 10 shows the anisotropic distribution of surface roughness length for the 12 wind directions specified in 30° increments, starting from the north and proceeding clockwise. Different features in the land surface modify the surface drag as the winds rotate anti-cyclonically. The high upwind roughness “footprint” of the wetland forests along the eastern shore of Cape Lookout, indicated by the green-yellow-red colors, is particularly noticeable in the figure.

Under large-scale heavily forested canopies, the water is sheltered from the wind and very little downward vertical momentum transfer occurs – the water surface is effectively decoupled from the wind field. Therefore, when an ADCIRC model node's land cover type falls in the 41–43 or 90–93 NLCD categories (indicated in bold print in Table 3), its vegetation canopy coefficient (*VCanopy*) is set to zero in the nodal attributes input file and no wind stress is applied at the water surface.

5.2. Calculation of Manning's-n friction coefficients

The drag coefficient for the spatially varying bottom friction induced by flow over channel bed material is calculated using the equation

$$C_f = \frac{gn^2}{\sqrt[3]{H}}, \quad (7)$$

where *g* is the gravitational constant, *n* is the Manning's-n friction coefficient and *H* is the total height of the water column (depth plus surface elevation). The inclusion of this parameterization is crucial for improving predictions of inundation because it modulates the water velocity according to the land cover encountered during overwash and drainage situations. The Manning's-n formula is applied over the entire model domain. The total water depth, *H*, at every node is compared against a minimum water depth, *H*₀ (0.02 m). As long as *H* is larger than this minimum value, the node is considered “wet” and it remains active. However, if the total water depth falls below this minimum value, then the node is deemed “dry” (inactive) and it is not used in the calculations. A minimum background value of *n* = 0.02 is used in the non-inundation portion of the computational grid domain.

Although the minimum distance separating computational grid nodes is 27 m and the resolution of the land cover data is 30 m, only a small fraction of the model's triangular elements are of similar size. An analysis of the grid's finite-element size distribution over land in the inundation portion of the high-resolution NC grid indicated that using a 5 × 5 spatial average of NLCD cell values would produce estimates of the Manning's-n friction coefficient that are most consistent with the mean resolution of the grid. Therefore, the average Manning's-n friction coefficient was computed from

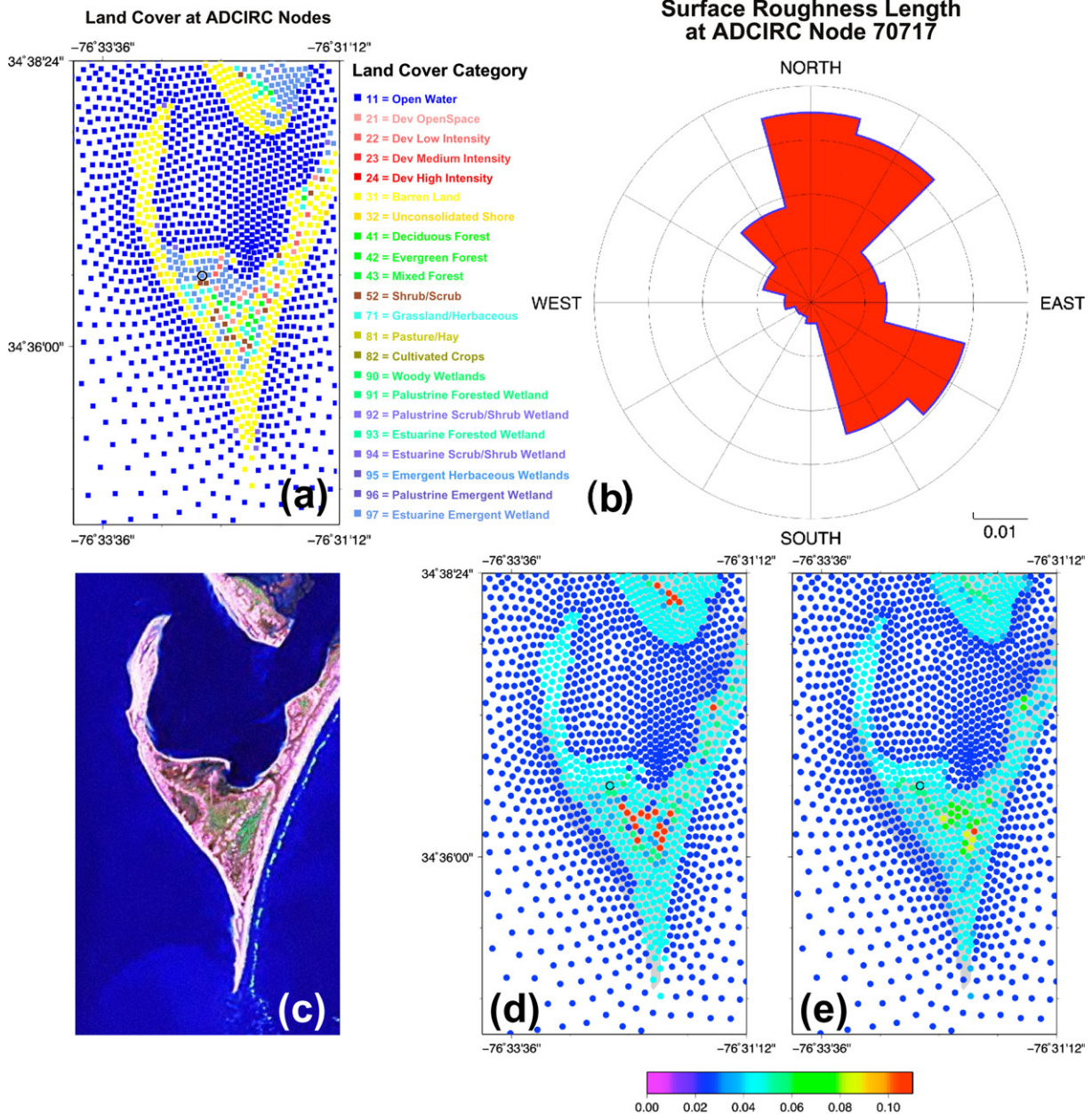


Fig. 9. (a) Categories of land cover at ADCIRC model grid nodes over Cape Lookout, NC, with node #70717, located in the center of the figure, circled, (b) polar coordinate "rose" plot of the surface roughness length (m) as a function of wind direction at ADCIRC model node #70717, (c) satellite image of Cape Lookout, NC (Landsat imagery courtesy of NASA's Stennis Space Center), (d) cell Manning's-n friction coefficient and (e) average Manning's-n friction coefficient over Cape Lookout, NC.

5×5 land cover cell windows ($150 \times 150 \text{ m}^2$). An example of the cell Manning's-n (the value in the pixel in which the node is located) and average Manning's-n coefficients over Cape Lookout, in the vicinity of ADCIRC model node #70717 (circled), are shown in Fig. 9d and e. As expected, the averaged Manning's-n friction coefficient values are smoother than the cell values.

6. Improved storm surge simulation results

A retrospective test case, Hurricane Ophelia (2005), was used to evaluate the impact of the new asymmetric winds forcing and the recently incorporated model enhancements (surface roughness length, forest canopy and Manning's-n friction coefficient) on the predicted storm surge. Hurricane Ophelia's track is shown in Fig. 11a and the recorded sea surface elevation for the NOAA/NOS/CO-OPS station at Wrightsville Beach, NC is shown

in Fig. 11b. The storm formed on September 4, 2005 near the Bahamas from the remnants of a cold front in an elongated trough of low pressure. Due to the presence of weak steering currents, its motion was slow and erratic. It made several clockwise and counterclockwise loops during its gradual trek northward. Ophelia's intensity oscillated between tropical storm and hurricane strength until its fourth re-intensification off the NC coast, where it reached its peak intensity of 75 kt (38.6 m/s) on September 14–15. Although it never made landfall, the northern portion of Ophelia's eye impinged on Cape Fear as it drifted in an east-northeast direction parallel to the NC coast from Wilmington to Morehead City, pummeling the coastline with high winds for 2 days. An upper-level trough associated with a cold front caused an abrupt change in Ophelia's track near Cape Hatteras on September 16 and swept the storm northward towards Massachusetts.

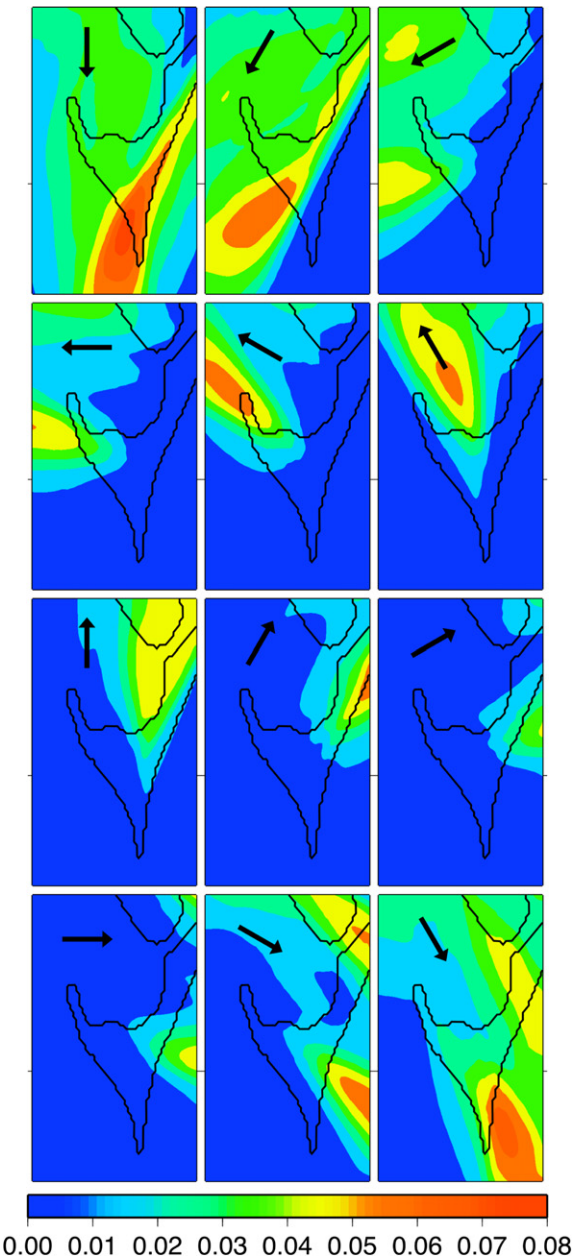


Fig. 10. Anisotropic distribution of surface roughness length over the Cape Lookout area for the 12 wind directions specified in 30° increments, starting from the north and proceeding clockwise.

Storm surge simulations were run with different methods of (1) *initialization*: cold start mode (with no tides) and hot start mode (starting with the tides-only hot start file then continuing with the daily tides), (2) with different *nodal attributes*: with/without the Manning's-n friction coefficients (Mn) and surface roughness length plus canopy effect (Sr) and (3) with different *wind forcing data*: the operationally released NHC forecast advisory data and the best track data obtained from NHC.

6.1. Effects of initialization: cold start vs. hot start

In order to determine how the incorporation of tides impacts the surge results, two cases were run: (1) a cold start (no tides) simulation for a period of 6.125 days, and (2) a hot start simu-

lation starting with the tides-only hot start file at 0:00 UTC September 11, 2005, then driven with the synthetic asymmetric winds and tidal forcing. To create a hot start file with tides for the Hurricane Ophelia case, the open boundary tidal conditions and interior tidal potential terms valid at 0:00 UTC June 1, 2005 were generated. The tides were simulated for 102 days from 0:00 UTC June 1, 2005 until 0:00 UTC September 11, 2005. Once the model was spun up with the tides-only runs, the synthetic asymmetric wind forcing was incorporated based on Hurricane Ophelia's wind parameters (eye location, highest sustained wind speed, 64/50/34 kt radii information, central pressure) from the advisories, driving the model from 0:00 UTC September 11 to 3:00 UTC September 17, 2005. For cold start mode, the same wind forcing was incorporated but no background tidal forcing was specified. In both cases no nodal attributes were used.

Fig. 12a and **b** show the predicted sea surface elevation and currents for the cold start simulation and the hot start simulation with tides, respectively, from the ADCIRC model valid at 22:30 UTC on September 14, 2005. The tideless cold start surge along the coast north of the storm reaches 0.6 m (1.97 ft) and the drawdown along the southern part of the coast is between -0.3 and -0.4 m (-0.98 and -1.31 ft). In contrast, the hot start run produces values greater than 1.2 m (3.94 ft) along the coast on the northern side of the storm. The cold start reached a maximum surface elevation of 2.19 m (7.19 ft) in the lee of the barrier islands, while the hot start simulation with the tides included produced a lesser maximum of 2.17 m (7.12 ft) at the same location. The observed sea surface height nearby, at the NOAA Beaufort tidal station, was 1.47 m (4.82 ft). However, there is a strong sea surface height gradient in the area between the islands and the coast in this area, which could account for the difference. The surface currents exhibit the same general pattern in both cases, with strong currents flowing towards the southwest along the NC coastline. There are also differences in Pamlico Sound, where the hot start simulation predicts much stronger currents penetrating through the inlets between the barrier islands.

The surge above tides was calculated by removing the tides from the sea surface elevation after the fact (**Fig. 12d**) for Hurricane Ophelia at 22:30 UTC Sept 14, 2005 for the hot start simulation, then compared against the cold start sea surface elevation (**Fig. 12c**, same as **Fig. 12a** but displayed with a different color range and no surface currents for better comparison) at the same forecast time. As mentioned before, the cold start surge maximum of 2.19 m (7.19 ft) is localized at an area in the lee of the barrier islands, while the hot start run surge maximum is in the same location but the value is much lower (1.30 m or 4.27 ft) since the tides have been removed. The observed surge above tides at the NOAA Beaufort tidal station was 0.86 m (2.82 ft). Surge values greater than 0.6 m (1.97 ft) in the hot start run extend across a wider area of the NC coast than in the cold start run, as seen in the difference between the surge above tides and the cold start (**Fig. 12e**). Differences between the two simulations exceed 10 cm (3.94 in) along most of the southeastern portion of the NC coast. At some locations, such as the Cape Fear River and Beaufort Inlet areas, differences are greater than 30 cm (11.81 in). The drawdown in the cold start simulation is more severe. In Pamlico Sound, the hot start produces a lower sea surface elevation above tides in the lee of the barrier islands and throughout the sounds. This shows that tides have a nonlinear impact on the sea surface elevation near the coastline – they cannot be added *a posteriori* to the cold start sea surface elevation after the simulations are conducted, but need to be included in the boundary and interior forcing at the outset and through the duration of the simulations.

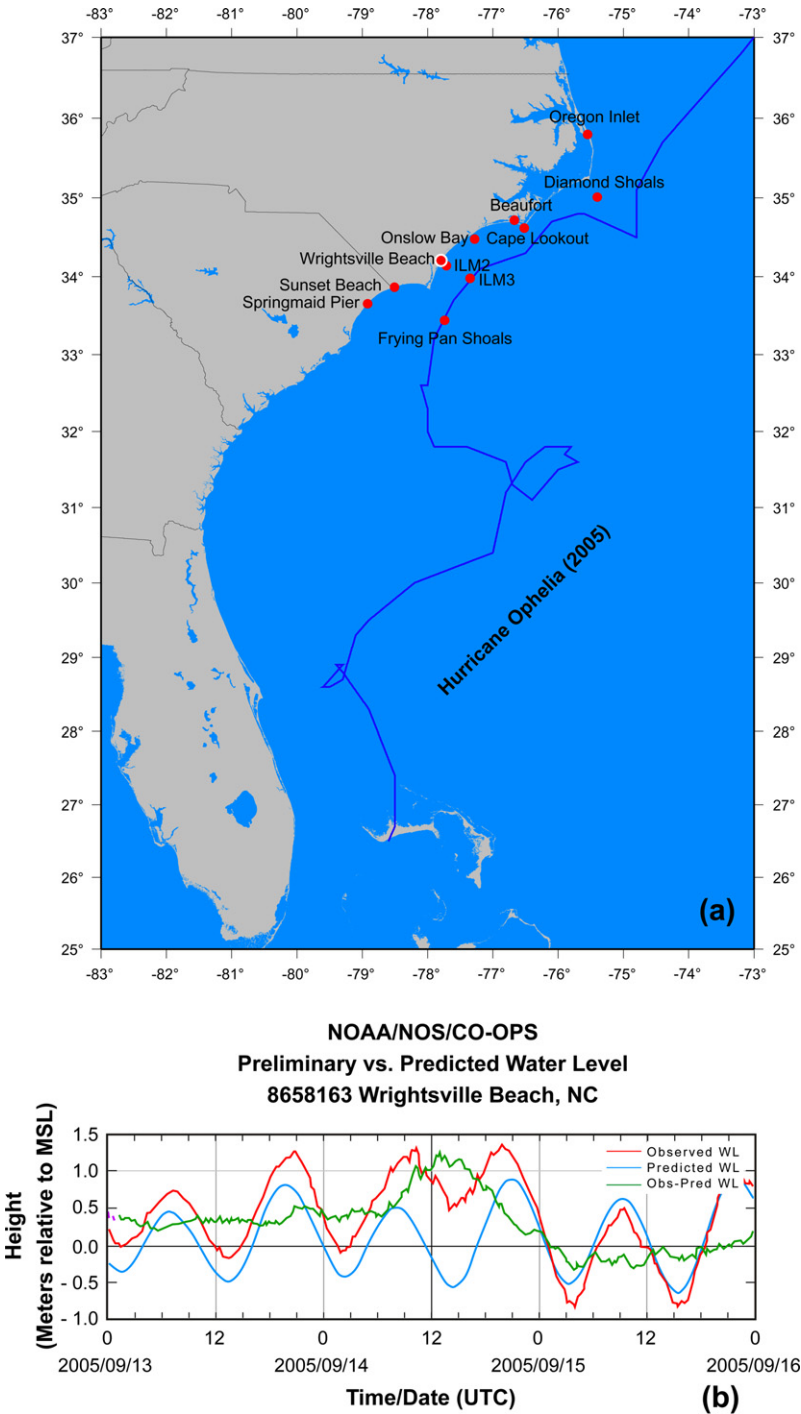


Fig. 11. (a) Track for Hurricane Ophelia from September 6–17, 2005. Data from the NHC advisories for this period were used to drive the ADCIRC storm surge prediction model. Observations from the stations shown were used to validate the model. (b) Recorded sea surface elevation for the NOAA/NOS/CO-OPS station at Wrightsville Beach, NC.

6.2. Effects of nodal attributes: Mn and Sr vs. $NoMn$ and $NoSr$

Simulations with Manning's-n friction coefficient (Mn) and surface roughness length plus a forest canopy coefficient (Sr) were conducted. Fig. 13a and b show the 10-min averaged winds at 22:30 UTC on September 14, 2005 used in the Hurricane Ophelia storm surge simulations run with and without these nodal attributes.

Note in Fig. 13a that there is no difference in strength between the winds offshore and those over land. This is unrealistic since

winds normally diminish exponentially inland with increased surface roughness (Kaplan and DeMaria, 1995). Fig. 13b shows the winds with both the surface roughness length effects and canopy nodal attributes. The surface canopy coefficient in ADCIRC is set to 0 where the wind stress should be zero due to sheltering from forest canopy, and 1 otherwise. The wind speeds are dramatically reduced inland.

Zooming in on a coastal area reveals detailed, land cover-dependent structures in the horizontal distribution of the winds (Fig. 13c and d). Small notches are cut into the isolachs (Fig. 13c) in the

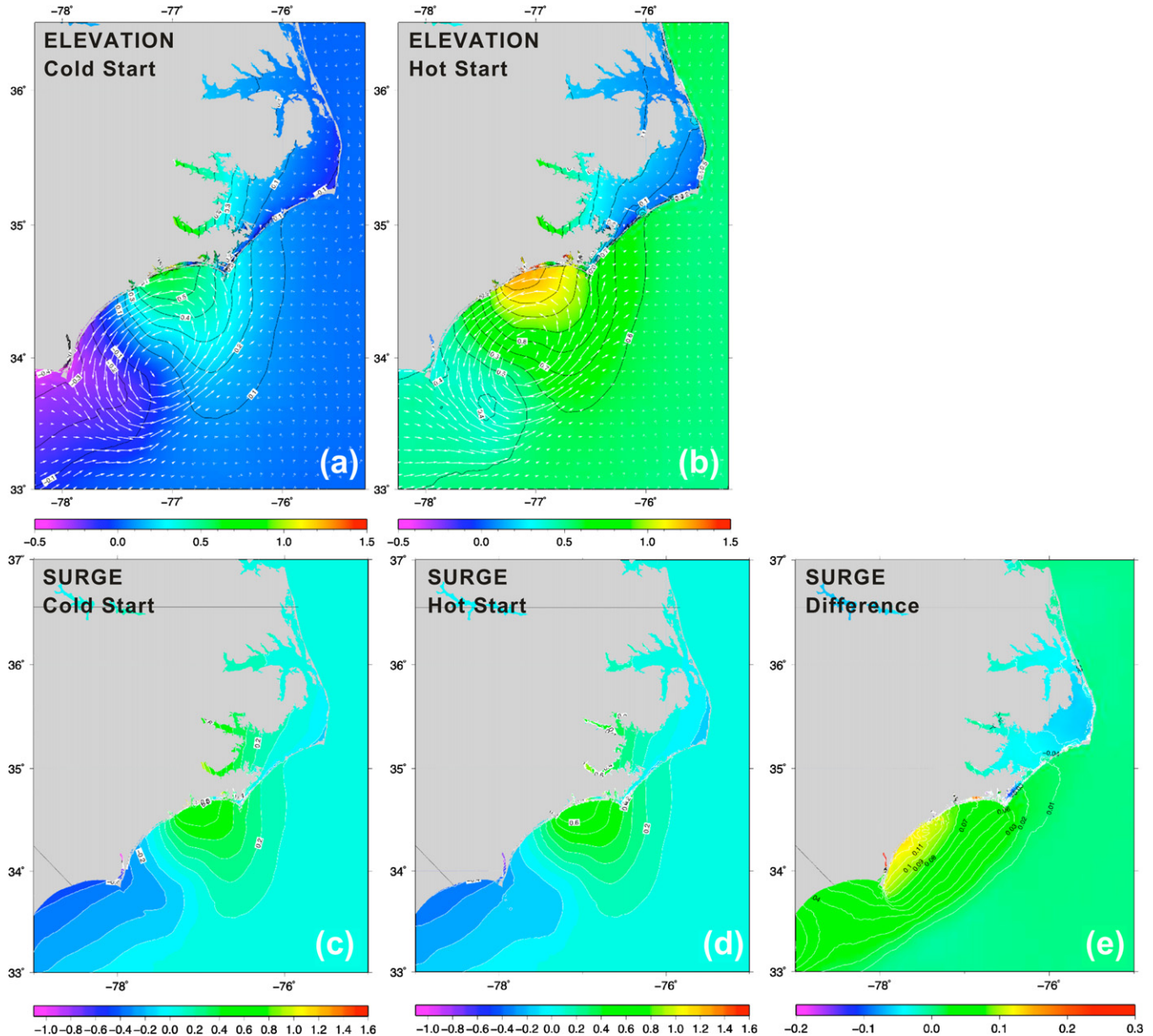


Fig. 12. Sea surface elevation (m) and surface currents (m/s) from the ADCIRC model at 22:30 UTC on September 14, 2005 using NHC advisory derived winds: (a) cold start without nodal attributes (no Mn , no Sr) and (b) hot start without nodal attributes (no Mn , no Sr). The impact of the hot start initialization is displayed in the (c) cold start, (d) hot start and (e) difference in the surge above tides (m) from the ADCIRC model simulation valid at 22:30 UTC on September 14, 2005.

immediate lee of the barrier islands, while complex acceleration/deceleration patterns occur where the land transitions from low-drag regions, such as the large cardioid-shaped area of cropland (indicated by the lighter blue color, 30+ knot winds) northeast of Beaufort, NC, to the high-drag forested areas downwind (darker blue color). Channeling up the Neuse River between the tree-lined banks is also clearly evident in the figure (cyan colored patches). This depiction is much more realistic and consistent with what really occurs when high winds are modulated by variations in the surface roughness. Thus, the synthetic asymmetric wind model, when enhanced with the upwind exposure wind drag formulation used in ADCIRC, successfully replicates a horizontally heterogeneous, surface characteristics-modified inland decay of wind speed.

The sea surface elevation and surface currents for ADCIRC simulations run with Mn and Sr are shown in Fig. 14a. The sea surface currents follow the counterclockwise pattern of the hurricane

winds, which causes the water to pile up along the NC coast north of the storm's eye and be evacuated southwest of the storm's center. The sea surface elevation is higher at the coast when Mn and Sr are activated. In the case without Mn and Sr (Fig. 14b), the overestimated drawdown southwest of the hurricane was produced by erroneously high offshore winds in the absence of land cover-enhanced drag.

The sea surface elevations with and without Mn and Sr were compared by calculating the difference field (Fig. 14c). Three distinct patterns are apparent. First, the difference field shows the impact of the Manning's-n friction parameterization in shallow water, evidenced by the higher values of sea surface elevation in the location of the eye, but no effect in deeper water. Second, the surface roughness effect is seen in the southern part of NC where the winds offshore produce less of a drawdown with these nodal attributes activated than without. In Pamlico Sound, where the winds diminished in the $Mn + Sr$ case, the difference is negative

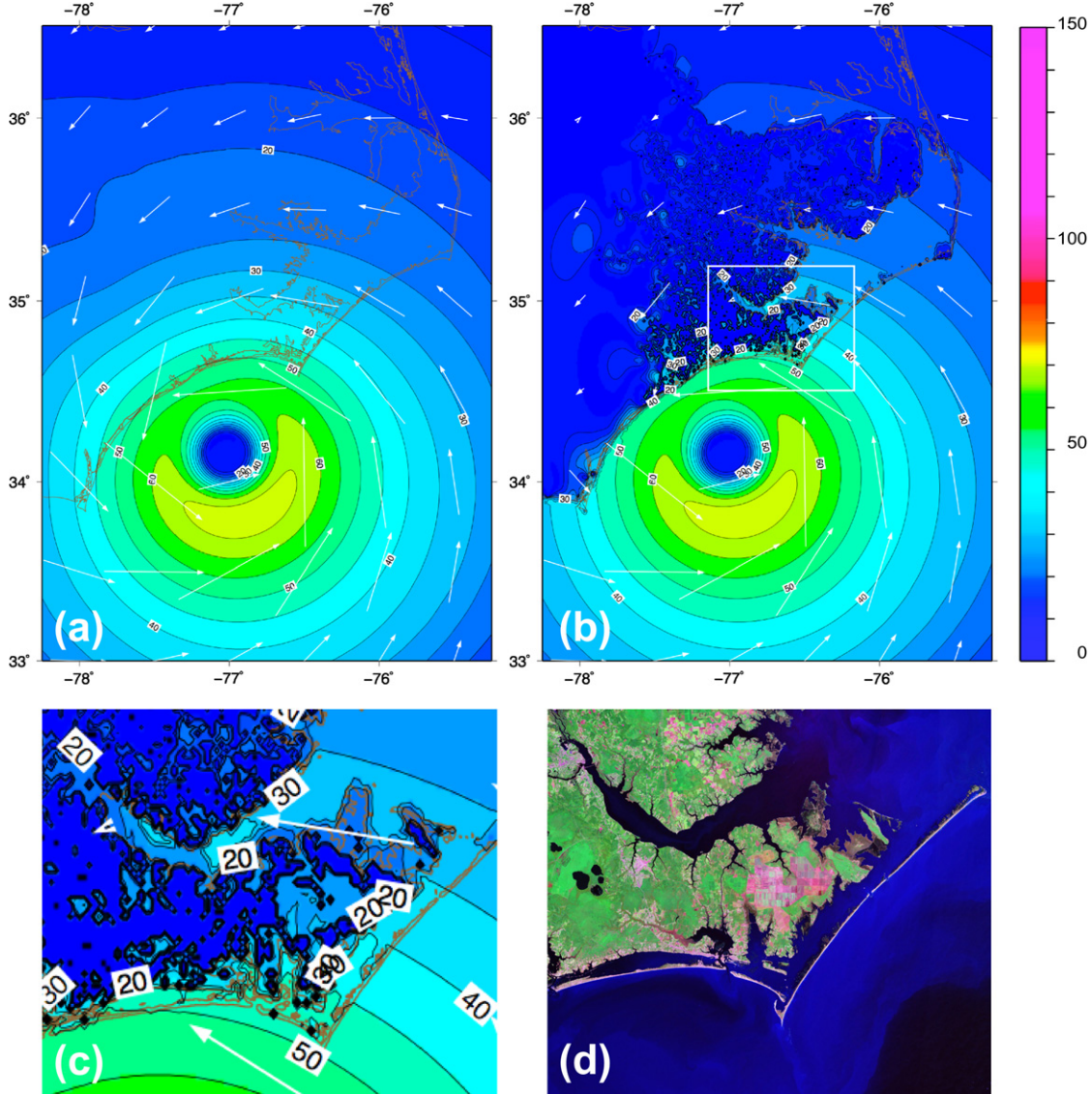


Fig. 13. 10-Minute averaged winds (kt) from the ADCIRC model at 22:30 UTC on September 14, 2005 (a) with neither surface roughness nor tree canopy sheltering (no Sr), (b) with both surface roughness and tree canopy sheltering (Sr), (c) zoomed area from white box in panel (b), and (d) satellite image over the geographical area in panel (c). (Landsat imagery courtesy of NASA's Stennis Space Center.)

since lighter winds cause less water to be driven against the mainland coast inside the sound than without Mn and Sr .

The NHC public advisory had predicted maximum coastal storm surge flooding of 5–7 ft (1.52–2.13 m) above normal tide levels, which is slightly higher than the values reported. According to the Tropical Cyclone Report (Beven and Cobb, 2005), Hurricane Ophelia caused storm surges of 4–6 ft (1.22–1.82 m) above normal tide levels in Pamlico Sound, including the lower reaches of the Neuse, Pamlico, and Newport Rivers and along the open coasts west of Cape Lookout. Surges of 3–4 ft (0.91–1.21 m) above normal tide levels were observed in other affected areas along the North Carolina coast. The modeled maximum surge above tides from the simulation with Mn and Sr (Fig. 14d) reached 1.21 m (3.96 ft), in very good agreement with the reported values.

In Pamlico Sound, stronger incoming currents flow through the inlets in the case without Mn or Sr (Fig. 14b) than with Mn and Sr (Fig. 14a), resulting in higher water surface elevations. Fig. 14e shows that for the same simulation with Sr but no Mn , the storm surge pattern in Pamlico Sound is very similar to the simulation with no Mn and no Sr (Fig. 12d), indicating that the lower surge

(Fig. 14d) is due to the inclusion of a spatially varying Manning's-n friction coefficient. Further investigation, including calculations of the mass transport through the inlets and channels, should be conducted to account for this difference.

Though Hurricane Ophelia never made landfall in North Carolina, its winds opened a new inlet three-fourths of a mile (1.2 km) south of New Drum Inlet. The hurricane also significantly widened Old Drum Inlet, which had been almost closed, as storm surge washed over the entire length of the Cape Lookout National Seashore (Beavers and Selleck, 2005).

To further analyze the impact of the inclusion of nodal attributes on inundation, analyses were conducted over a smaller area in northern North Carolina where the grid resolution is the highest. It is particularly noticeable that the no nodal attributes simulations (Fig. 15a) produced stronger currents and more flooding than those that included nodal attributes (Fig. 15b). A surface elevation above 1 m (3.28 ft) (yellow color in Fig. 15a) pushes far up the Neuse River into New Bern in the simulation without nodal attributes. This overprediction is remedied when nodal attributes are included (green color re-

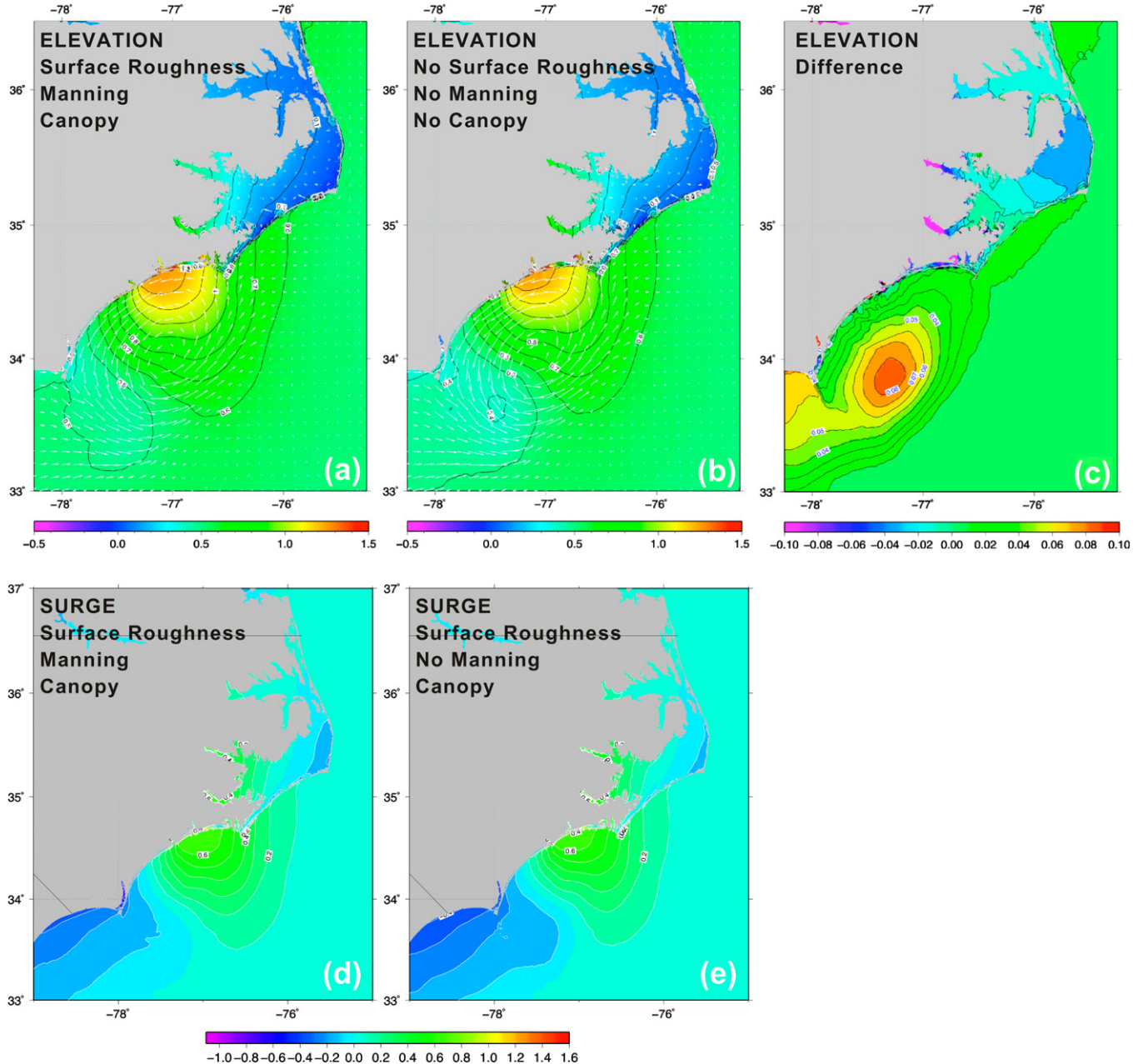


Fig. 14. Impact of nodal attributes. Sea surface elevation (m) and surface currents (m/s) from ADCIRC model simulation valid at 22:30 UTC on September 14, 2005 (a) with surface roughness, Manning's-n friction coefficient and forest canopy, (b) without any of these nodal attributes, (c) the computed difference, (d) surge above tides (m) with Manning's-n friction coefficient (Mn) and surface roughness and canopy (Sr) and (e) with surface roughness and canopy (Sr) only.

places yellow in Fig. 15b). The higher west-southwest directed current velocities along the coast west of Cape Lookout, in the case of no Manning's-n friction coefficient and no surface roughness, cause a higher surge through the inlets, in the sounds and along creek/river banks. There are also faster currents on the sound side of the barrier islands due to pure unmodulated marine winds acting in the absence of a surface roughness parameterization and the lack of an underwater drag enhancement. Simulations without (with) Mn and Sr produce velocities of 1.58 m/s (1.34 m/s) and 1.25 m/s (1.04 m/s) to the north and south of Ocracoke Island.

The maximum elevation reached in the simulation at each node both without and with including the land cover-derived surface roughness length, the forest canopy sheltering effect and the Manning's-n friction coefficient as nodal attributes is shown in Fig. 15c

and d, respectively. Fig. 15c displays higher inundation values that spread over larger areas than in Fig. 15d. This excessive flooding is very noticeable, with high values extending westward along the interior shoreline of the sounds and further up the rivers in Fig. 15c compared to Fig. 15d. In the northern part of the state, there is more inundation in the marsh areas along the rivers and canals when the roughness parameterizations are deactivated. In both figures, surge pushes up the rivers and floods the agricultural areas from both the north and south. The maximum elevation reached in the simulation with no nodal attributes is 3.11 m (10.2 ft) while the flooding produced in the simulation with nodal attributes reached only 2.72 m (8.92 ft) in the agricultural areas when the hurricane was located due east offshore. The NC Department of Crime Control and Public Safety reported storm surges of 7–12 ft (2.1–3.6 m) in the shallow inlets of Pamlico Sound.

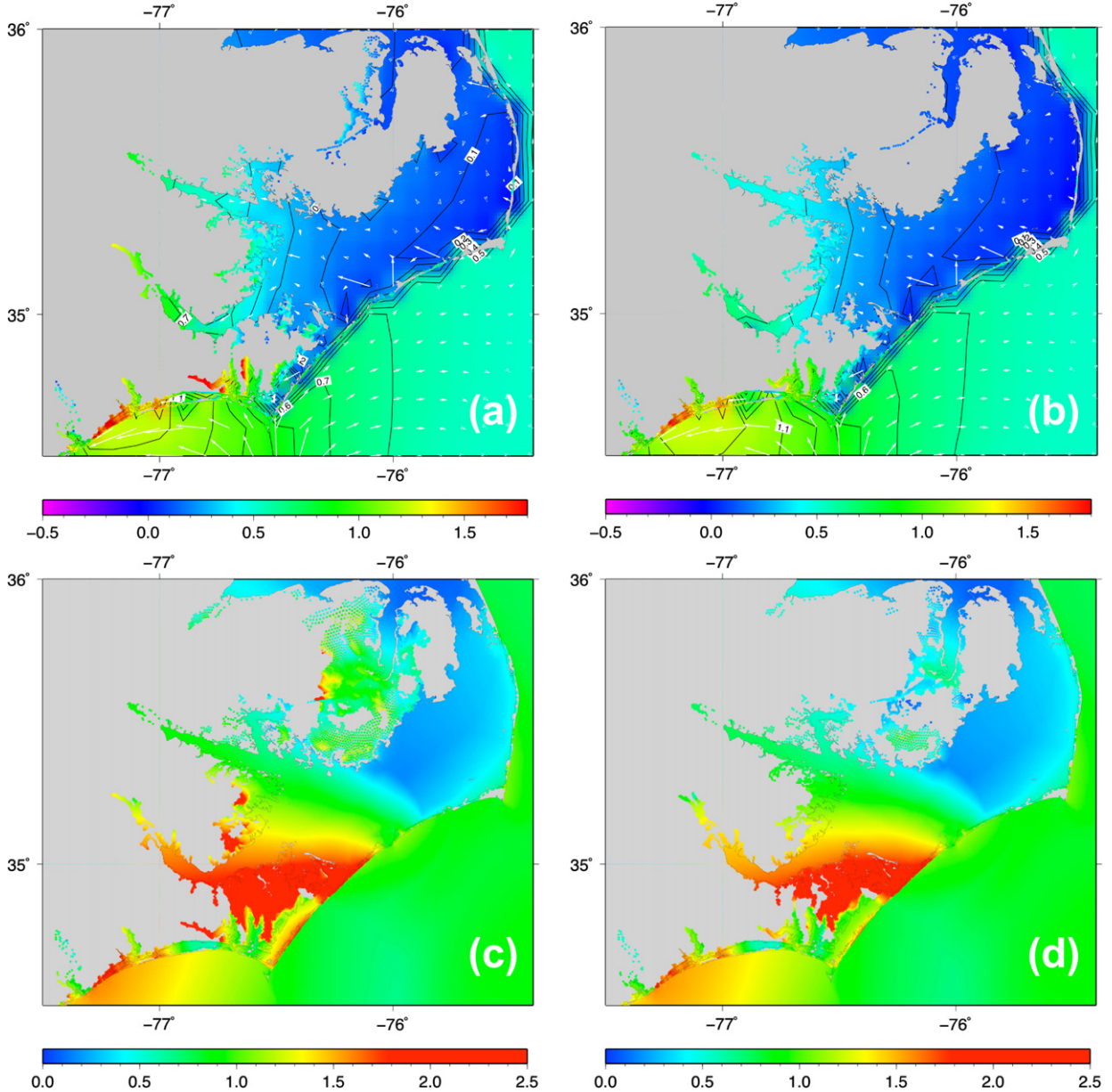


Fig. 15. (a) As in Fig. 14b without nodal attributes. (b) As in Fig. 14a, with the nodal attributes Manning's-n friction and surface roughness specified, but zooming in on the northern NC coastal area to reveal details in the inundation. Maximum elevation reached during the entire simulation (c) without nodal attributes (d) with nodal attributes. Larger inundation areas are predicted without nodal attributes.

6.3. Effects of wind forcing: best track vs. NHC advisory derived winds

Fig. 16a shows the sea surface elevation from a $Mn + Sr$ simulation but forced with the corrected best track winds. The sea surface heights driven by the best track winds are about 10–20 cm (3.9–7.9 in) lower than in the simulation forced with the wind data from the operational NHC advisories. The magnitude of the sea surface elevation in the return flow region along the coast is also slightly smaller than the one produced by NHC derived winds. Likewise, the storm surge up the coast (Fig. 16b) generated by the best track wind data is slightly lower in magnitude than in the simulation driven by the NHC advisory derived winds. The difference in storm surge between the best track and NHC simulation can be explained by the differences in the wind radii reported in the data. The best track storm shape, derived from the wind radii, is more elongated in the northeast and southeast directions so the winds are diminished along the NC coastline. This produces an attenuated storm surge.

6.4. Comparison between observed and asymmetric vortex winds

To assess the performance of the parametric model, the asymmetric winds for Hurricane Ophelia were compared with station wind observations. Time series analysis, root mean square (RMS) error and correlation calculations were conducted. Fig. 17 displays a comparison between the observed and ADCIRC wind speeds and phases, together with the RMS errors and correlations computed at the meteorological station locations shown in Fig. 11.

RMS errors in the wind speed range from 3.35 m/s (6.51 kt) at Wrightsville Beach to 6.25 m/s (12.15 kt) at Cape Lookout. The passage of the eye of Hurricane Ophelia directly over Frying Pan Shoals is captured extremely well by the parametric wind model. The two sides of the eye are clearly visible in Fig. 17i. The steepness of the eyewall is nearly perfect. The asymmetric vortex representation slightly overshoots the wind intensity at the radius of maximum winds, suggesting that the Holland shape parameter B could be adjusted downward by a small amount. Although Ophelia's approach

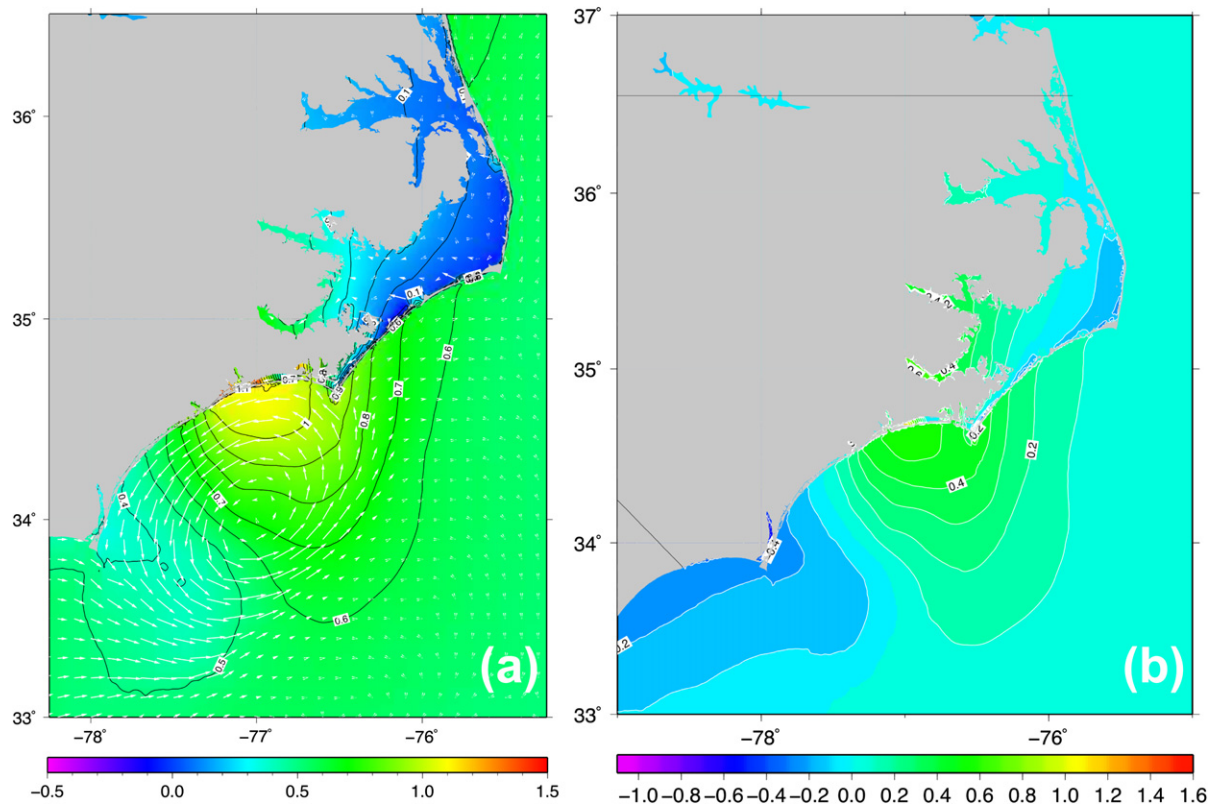


Fig. 16. (a) Sea surface elevation (m) and surface currents (m/s) and (b) surge above tides (m) with Manning's-n friction coefficient (M_n) and surface roughness (S_r) from the ADCIRC model at 22:30 UTC on September 14, 2005 using best track derived winds.

towards Cape Lookout on September 14 is quite realistic, the simulated storm remains too far offshore. There is a hint that the storm's center is nearby, but the wind speed trace does not replicate the abrupt falloff to 7 m/s (13.6 kt) recorded within the eye. In general, the simulation of wind direction is remarkable, given that the asymmetric wind vortex employs an idealized frictional inflow parameterization. The ADCIRC winds increase too soon and decay too rapidly at Diamond Shoals, as Hurricane Ophelia jogs southeastward away from the coastline before it pivots and accelerates towards the northeast. The strongest reported winds were from the C-MAN station at Cape Lookout, which reported 2-min averaged winds of 65 kt (33.4 m/s) on September 14 with a gust to 80 kt (41.2 m/s). The National Ocean Service (NOS) station at Wrightsville Beach reported 6-min averaged winds of 59 kt (30.4 m/s) (Beven and Cobb, 2005).

6.5. Comparison between observed and model predicted water elevations

Tidal station data were extracted from the NOAA web site (http://tidesandcurrents.noaa.gov/station_retrieve.shtml?type=Tide+Predictions) for all stations along the NC and SC coasts. An example of the Wrightsville Beach record is shown in Fig. 11b.

Fig. 18 compares the simulated sea surface height elevation against the recorded NOAA/NOS tidal station data (left panels) at several station locations. The RMS error between the observed and modeled sea surface height values range from 10 to 40 cm (3.9–15.8 in) while the correlations are between 0.87 and 0.98. The observed and modeled tides are shown in the center panels. The RMS error between the observed and modeled tides range from 6 to 13 cm (2.4–5.1 in) while the correlations are between 0.96 and 0.99. The elevation due solely to tides was removed from

the total sea surface elevation and the predicted tides were subtracted from the observed sea surface elevation at each NOAA tidal station to obtain the modeled and observed surge (right panels). The RMS error between the observed and modeled surge ranges from 8 cm (3.1 in) at Oregon Inlet to 36 cm (14.2 in) at Beaufort while the correlations range between 0.67 and 0.94. The largest discrepancy occurs at the Beaufort station, probably due to the grid resolution, bathymetry and the intricate geometry in that particular area. Efforts are underway at UNC-IMS to improve the grid and the bathymetric representations through the inlets and along the intracoastal waterways. The hurricane surge signal can be seen propagating from south to north (bottom to top) in time in the right panels of the figure. The drawdown is noticeable in the time series at the southern stations (Fig. 18o and l), while the surge is highest at Wrightsville Beach and Beaufort. The Wrightsville Beach NOS station recorded a surge of 4.13 ft (1.26 m) and Sunset Beach CARO-COOPS station recorded 2.72 ft (0.83 m). [Beven and Cobb (2005) reported storm surge values of 4.19 ft (1.28 m) and 2.85 ft (0.87 m), respectively.] The ADCIRC simulation produced a surge above tides of 1.15 m or 3.77 ft (a difference of 11 cm or 4.3 in) at Wrightsville Beach (Fig. 18i) and 0.72 m or 2.36 ft (a 11 cm or 4.3 inch difference) at Sunset Beach (Fig. 18l).

The current accuracy of the SLOSH model, computed as the fractional difference between the simulated peak surge and the observed peak surge, is about $\pm 20\%$ (OFCM, 2007). In the ADCIRC simulations of Hurricane Ophelia, the best performance achieved was at Springmaid Pier (−4%), Wrightsville Beach (−9%), where the highest storm surge occurred, and Sunset Beach (−16%). Unfortunately, due to isolated defects in the finite-element grid mesh, the predicted surge at soundside stations located in shallow water (Oregon Inlet and Beaufort) was not very accurate. The resolution

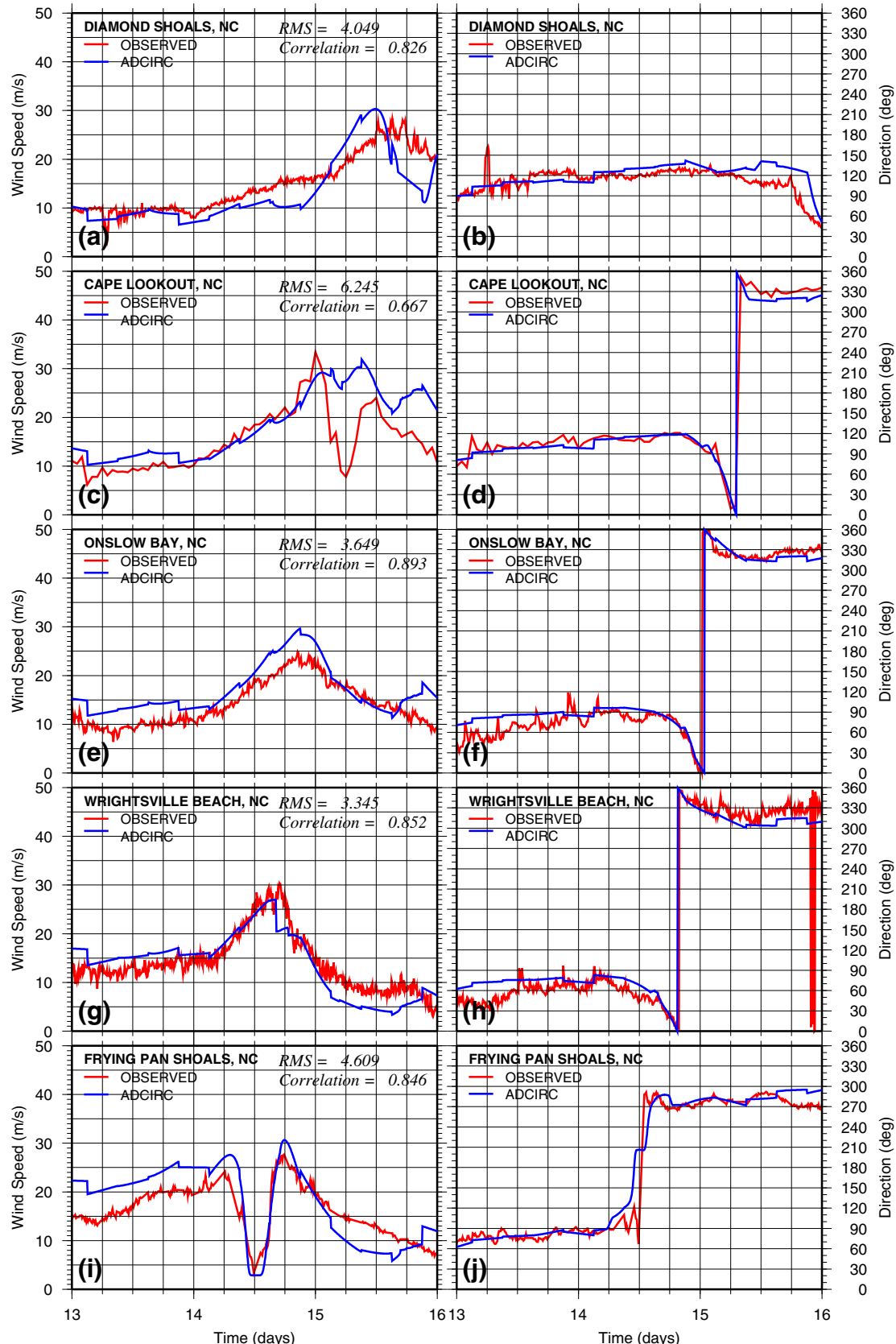


Fig. 17. Comparison of ADCIRC vs. observed time series of wind speed (m/s) (left panels) and direction (degrees clockwise from North) (right panels) during Hurricane Ophelia (2005) at five coastal stations in North Carolina: (a,b) Diamond Shoals Light, (c,d) Cape Lookout, (e,f) Onslow Bay, (g,h) Wrightsville Beach and (i,j) Frying Pan Shoals Light. The hurricane's track and the station locations are displayed in Fig. 11.

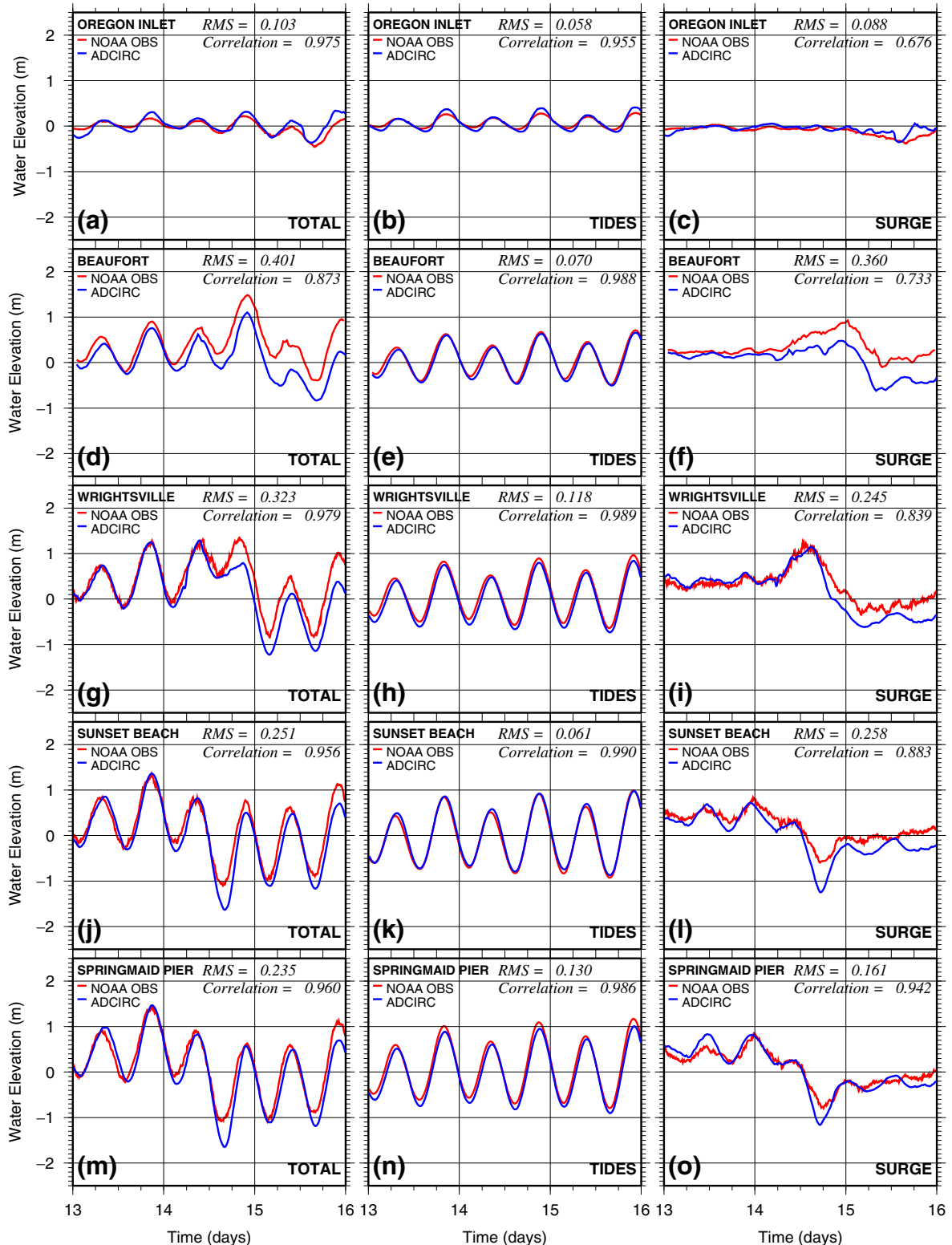


Fig. 18. Observed, predicted and observed minus predicted sea surface elevation (m) at Oregon Inlet, Beaufort, Wrightsville Beach, Sunset Beach and Springmaid Pier during Hurricane Ophelia from NOAA/NOS/CO-OPS data (red) and ADCIRC (blue). (For interpretation of the references to colour in this figure legend, the reader is referred to the web version of this article.)

of the grid and the bathymetry in these problematic areas are currently undergoing refinement.

An interesting progression of events occurred in the sounds during the passage of the storm. Fig. 18b shows a comparison between the NOAA tides and the ADCIRC modeled tides at Oregon Inlet station, while Fig. 18a shows the actual NOAA observed

sea surface height vs. the ADCIRC model sea surface elevation. As Hurricane Ophelia approached, the fetch pushed the water westward across the sound, leaving boats stranded on dry ground and channel markers exposed. Fig. 18c shows the drawdown (negative surge). Later, when Ophelia pulled off to the east into the open Atlantic and the setup relaxed, a small compensatory,

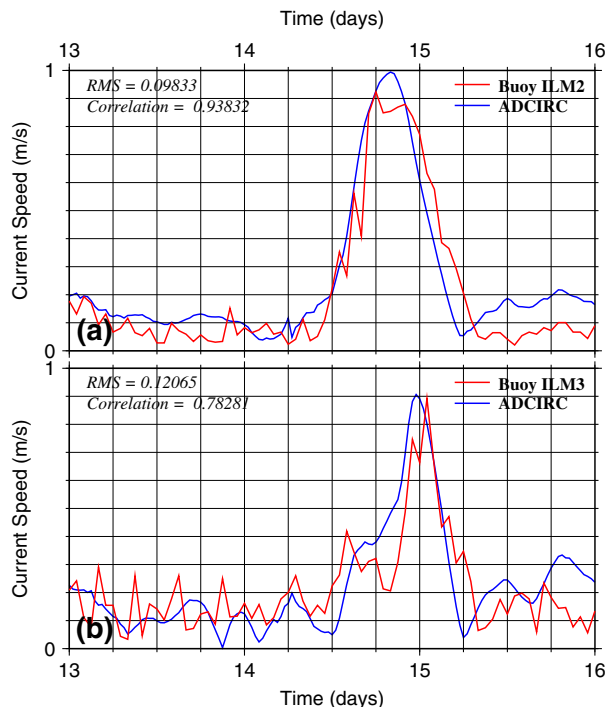


Fig. 19. Comparison between the ADCIRC depth-averaged current velocity (blue) and the average of the surface and bottom velocities measured by Acoustic Doppler Current Profilers (ADCPs) maintained by the Coastal Ocean Research and Monitoring Program (CORMP) at two stations off the North Carolina coast: (a) ILM2 and (b) ILM3 (locations shown in 11).

return-flow surge was produced in the left/rear quadrants of the hurricane.

6.6. Comparison between observed and model predicted current velocities

Fig. 19 shows a comparison between the ADCIRC depth-averaged current velocity and the average between the surface and bottom velocities measured by Acoustic Doppler Current Profilers (ADCPs) maintained by the Coastal Ocean Research and Monitoring Program (CORMP) at two stations off the North Carolina coast, ILM2 and ILM3 (locations shown in Fig. 11a). The modeled current velocities are in good agreement with the observed values. The maximum observed velocities at ILM2 and ILM3 are 0.92 and 0.89 m/s (1.79 and 1.73 kt), respectively, while the simulated velocities are 0.99 and 0.90 m/s (1.92 and 1.75 kt) at those stations. The RMS error values are 9–12 cm/s (0.17–0.23 kt) and the correlations are between 0.78 and 0.93. Both stations show a hint of the eye of the hurricane in the observations but not in the modeled velocities. One plausible explanation is that the Ophelia's eye passed close enough to the station to lower the velocities but, since the analytical model is based on eye fixes and the eye crossed the station in-between hurricane forecast advisories, the temporal frequency of the guidance is not high enough to resolve the exact track of the storm between hurricane forecast advisories given 6 h apart. A small temporary wobble in the track could account for the difference in the time series trace.

7. Conclusions

Substantial progress has been achieved in developing a new real-time, event-triggered storm surge prediction system for the State of North Carolina to assist emergency managers with evacuation planning, decision-making and resource deployment during

tropical storm landfall events. Based on a high-resolution, two-dimensional, depth-integrated version of the ADCIRC coastal ocean model and driven by winds from a synthetic asymmetric gradient wind vortex generated from real-time National Hurricane Center (NHC) forecast advisories, the prototype NCFS produced remarkably realistic predictions of storm surge during its first two years of deployment.

The key advantage of employing these parametric wind fields in the operational forecast system is that there is no need to wait for the NOAA/NCEP numerical weather prediction models to finish running, nor to download and process the gridded wind and pressure fields, all of which would delay the storm surge forecast by several hours. As soon as NHC's advisories hit the Family of Services real-time weather data stream in the LDM, the forecast is automatically triggered. This makes the NCFS well-suited for predicting storm surge even in the most difficult cases, when the tracks are erratic and the NHC forecast eye positions fluctuate up until the last minute.

The quality of the storm surge forecasts, as measured by the mean RMS error and correlation in the predicted sea surface elevation at NOAA tidal station locations, is promising, particularly in the near-field where the hurricane wind forcing overwhelms the background synoptic flow. Therefore, this quick-look, rapid-response forecast could serve as the first member of a storm surge prediction ensemble. It should be noted, however, that the storm surge predictions are quite sensitive to the storm wind parameters reported in the NHC forecast advisories, particularly the radii reported at standard wind intensities, which determine the shape of the isotachs.

Another advantage of the parametric synthetic vortex approach is that it provides infinite horizontal/temporal resolution, so the winds can be directly coupled to the ocean model at every finite-element node and computational time step while the model is running. The option of running simulations initialized with gridded numerical model winds or H*Wind analyses remains available to improve long-range predictions of storm surge and to provide better far-field fetch/wind forcing for wave models.

One other important finding is that, since tides have a non-linear effect on the sea surface elevation in coastal areas that can produce differences of up to 30 cm (1 ft) in the surge, it is imperative to include tidal forcing in the simulations. The tidal signal should not be added *a posteriori* to simulations without tides to try to recover the full elevation.

Now that the NCFS is running operationally, further scientific enhancements are currently underway. These include improving the wind forcing, extending the embedded high-resolution portion of the ADCIRC model grid inland/southward to encompass the entire NC coastline, incorporating topographic data from the NC Floodplain Mapping Program's 6-m resolution LiDAR DEM in this region, and conducting rigorous verification/calibration of the system's performance. A two-way coupling capability between ADCIRC and the Simulating WAves Nearshore (SWAN) shallow water wave model is currently under development. With the continued implementation of improvements such as these, this new forecast system offers the promise of minimizing the loss of life and structural damage that occurs in North Carolina during tropical storms.

Acknowledgements

This work was funded by the State of North Carolina through UNC-RENCI contract number 2-52130. The authors thank Rick Luettich, Crystal Fulcher and Jason Fleming at UNC's Institute of Marine Sciences in Morehead City, NC and Brian Blanton at RENCI in Chapel Hill, NC for their insights on ADCIRC model issues. Hurricane Specialists James Franklin and Lixion Avila and IT Specialist

Brian Maher at the National Hurricane Center were extremely helpful in providing detailed information about NHC's forecast products, their generation, timing and accuracy. Limei Ran processed the NLCD land use data for use in the ADCIRC nodal attributes file. John Atkinson contributed invaluable advice on the directional surface roughness algorithm and the calculation of the Manning's-n friction coefficients. Gopi Kandeswamy helped install the operational system at RENCI. The authors especially wish to thank Ken Galluppi, Manager of Emergency Management at RENCI, for his vision and management of this project.

References

- Arcement, G., Schneider, V., 1989. Guide for selecting Manning's roughness coefficients for natural channels and flood plains. United States Geological Survey Water Supply Paper 2339, USGS, 38 pp.
- Beavers, R., Selleck, J., 2005. Impacts to national parks from 2005 hurricane season coming to light: a preliminary overview. Natural Resource Year in Review – 2005. (http://www2.nature.nps.gov/YearinReview/00_B.html).
- Beven, J., Cobb, H.D., 2005. Tropical cyclone report Hurricane Ophelia, 6–17 September 2005. (http://www.nhc.noaa.gov/pdf/TCR-AL162005_Ophelia.pdf).
- Blain, C., McManus, A., 1998. A real-time application of the ADCIRC-2DDI hydrodynamic model for JTPIX97 at Camp Pendleton, CA. NRL/FR/7322-98-9684, Naval Research Laboratory, Department of the Navy, August 31, 1998.
- Blain, C., Rogers, E., 1998. Coastal tidal prediction using the ADCIRC_2DDI hydrodynamic finite element model. NRL/FR/7322-98-9682, Naval Research Laboratory, Department of the Navy, December 18, 1998.
- Blain, C., Westerink, J., Luettich, R., 1994. Domain and grid sensitivity studies for hurricane storm surge predictions. In: Peters, X.A., et al. (Eds.), Computational Methods in Water Resources, Heidelberg, July, 1994.
- Blake, E.J., Jarrell, E., Rappaport, Landsea, C., 2007. The deadliest, costliest, and most intense United States Tropical Cyclones From 1851 to 2006 (and other frequently requested hurricane facts). NOAA Technical Memorandum NWS TPC-5, NOAA/NWS/Tropical Prediction Center/National Hurricane Center, Miami, FL, 43 pp.
- Capitol Broadcasting Company, 2006. Time needed to evacuate the coast. Stormtracker – Your Official Hurricane Survival Guide, p. 2.
- Carteret County Shore Protection Office, 2007. Bogue Banks 2007 State of the Beach Report. Emerald Isle, NC.
- Dietsche, D., Hagen, S., Bacopoulos, P., 2007. Storm surge simulations for Hurricane Hugo (1989): On the significance of inundation areas. Journal of Waterways, Port, Coastal, and Ocean Engineering 133 (3), 183–191.
- Doodson, A., 1922. The harmonic development of the tide-generating potential. Proc. Roy. Soc. London, Ser. A 100, 305–329.
- Feyen, J., Hess, K., Spargo, E., Wong, A., White, S., Sellars, J., Gill, S., 2006. Flooding model to study sea level rise in North Carolina, Estuarine and coastal modeling. In: Proceedings of the 9th International Conference, Charleston, South Carolina, USA, October 31, 2006, pp. 338–356.
- Forbes, C., Fleming, J., Mattocks, C., Fulcher, C., Luettich, R., Westerink, J., Bunya, S., in press. New Developments in the ADCIRC community model, Estuarine and coastal modeling. In: Proceedings of the 10th International Conference, Newport, Rhode Island, USA, 20 pp. (in press).
- Graber, H., Cardone, V., Jensen, R., Slinn, D., Hagen, S., Cox, A., Powell, M., Grassl, C., 2006. Coastal forecasts and storm surge predictions for tropical cyclones: a timely partnership program. Oceanography 19 (1), 130–141.
- Hench, J.L., Luettich, R.A., 2003. Transient tidal circulation and momentum balances at a shallow inlet. J. Phys. Oceanogr. 33, 913–932.
- Holland, G.J., 1980. An analytical model of the wind and pressure profiles in hurricanes. Mon. Wea. Rev. 108, 1212–1218.
- Kaplan, J., DeMaria, M., 1995. A simple empirical model for predicting the decay of tropical cyclone winds after landfall. J. Appl. Met. 34, 2499.
- Luettich Jr., R., Hudgins, J., Goodall, C., 1996. Initial results from a combined tide and storm surge forecast model of the U.S. East Coast, Gulf of Mexico and Caribbean Sea. In: Proceedings of the 15th Conference on Weather Analysis and Forecasting, American Meteorological Society, Norfolk, VA, August 1996, pp. 547–550.
- Lynch, D., Smith, K., Blanton, B., Luettich Jr., R., Werner, F., 2004. Forecasting the coastal ocean: resolution, tide and operational data in the South Atlantic Bight. Journal of Atmospheric and Oceanic Technology 21 (7), 1074–1085.
- Mattocks, C., Forbes, C., Ran, L., 2006. Design and implementation of a real-time storm surge and flood forecasting capability for the State of North Carolina. UNC-CEP Technical Report, November 30, 2006, 103 pp.
- Mukai, A.Y., Westerink, J.J., Luettich Jr., R.A., Mark, D., 2002. Eastcoast 2001, A tidal constituent database for Western North Atlantic, Gulf of Mexico and Caribbean Sea. U.S. Army Corps of Engineers Technical Report ERDC/CHL TR-02-24, September 2002, 196 pp.
- Office of the Federal Coordinator for Meteorological Services and Supporting Research (OFCM), 2007. Interagency strategic research plan for tropical cyclones. The way ahead. (February, 2007). FCM-P36-2007, 270 pp.
- Powell, M., Houston, S., Amat, L., Morisseau-Leroy, N., 1998. The HRD real-time hurricane wind analysis system. J. Wind Engineer. Indust. Aerodyn. 53–64.
- Powell, M.D., Vickery, P.J., Reinhold, T.A., 2003. Reduced drag coefficient for high wind speeds in tropical cyclones. Nature 422, 279–283.
- Powell, M., Bowman, D., Gilhousen, D., Murillo, S., Carrasco, N., Fleur, R.St., 2004. Tropical cyclone winds at landfall: The ASOS-CMAN wind exposure documentation project. Bull. Amer. Met. Soc. 85, 845–851.
- Powell, M., Soukup, G., Cocke, S., Gulati, S., Morisseau-Leroy, N., Hamid, S., Dorst, N., Axe, L., 2005. State of Florida hurricane loss projection model: atmospheric science component. Journal of Wind Engineering and Industrial Aerodynamics 93 (8), 651–674.
- Queensland Government, 2001. Queensland climate change and community vulnerability to tropical cyclones: ocean hazards assessment – stage 1. J0004-PRO001C, The State of Queensland (Australia), Department of Natural Resources and Mines, Brisbane, Qld., 383 pp.
- Thompson, E., Cardone, V., 1996. Practical modeling of hurricane surface wind fields. J. Waterw. Port C-ASCE 122 (4), 195–205.
- Vickery, P., Skerlj, P., Steckley, A., Twisdale, L., 2000. Hurricane wind field model for use in hurricane simulations. J. Struct. Eng. ASCE 126 (10), 1203–1221.
- Westerink, J., 1993. Tidal prediction in the Gulf of Mexico/Galveston Bay using model ADCIRC-2DDI. Contractors Report to the US Army Engineer Waterways Experiment Station, Vicksburg, MS, January 1993.
- Westerink, J., Luettich Jr., R., Scheffner, N., 1993. ADCIRC: an advanced three-dimensional circulation model for shelves coasts and estuaries. Report 3: Development of a tidal constituent data base for the Western North Atlantic and Gulf of Mexico. Dredging Research Program Technical Report DRP-92-6, U.S. Army Engineers Waterways Experiment Station, Vicksburg, MS, 154 pp.
- Westerink, J.J., Luettich, R.A., Feyen, J.C., Atkinson, J.H., Dawson, C., Roberts, H.J., Powell, M.D., Dunion, J.P., Kubatko, E.J., Pourtaheri, H., 2008. A basin to channel scale unstructured grid hurricane storm surge model applied to Southern Louisiana. Mon. Wea. Rev. 136, 833–864.
- Westerink, J., Luettich, R., Baptista, A., Scheffner, N., Farrar, P., 1992. Tide and storm surge predictions using finite element model. ASCE J. Hydraul. Eng. 118 (10), 1373–1390.
- Williams, B., Meinhold, S., Routhail, N., Hummer, J., Tagliaferri, A., 2005. Traffic analysis of North Carolina's I-40 lane reversal plan – 2005 update. Presentation before the Transportation Research Board Emergency Evacuation Subcommittee, January 10, 2005.
- Xie, L., Bao, S., Petrasa, L.J., Foley, K., Fuentes, M., 2006. A real-time hurricane surface wind forecasting model: formulation and verification. Mon. Wea. Rev. 134, 1355–1370.